

https://dspace.org/

Comparative study of a time diversity scheme applied to G3 systems for narrowband power-line communications

Rivard, Yves-François

2016

http://hdl.handle.net/10539/22668

Rivard, Yves-François (2016) Comparative study of a time diversity scheme applied to G3 systems for narrowband power-line communications, University of the Witwatersrand, <http://hdl.handle.net/10539/22668>

Downloaded from a DSpace repository. https://dspace.org/



COMPARATIVE STUDY OF A TIME DIVERSITY SCHEME APPLIED TO G3 SYSTEMS FOR NARROWBAND POWER-LINE COMMUNICATIONS

A dissertation submitted to the Faculty of Engineering and the Built Environment, University of the Witwatersrand, Johannesburg, in fulfilment of the requirements for the degree of Masters of Science in Engineering (Electrical).

Yves-François Rivard - Student No. 479536
Research Supervisor: Prof. Ling Cheng

The financial assistance of the National Research Foundation (NRF) towards this research is hereby acknowledged. Opinions expressed and conclusions arrived at, are those of the author and are not necessarily to be attributed to the NRF.

Johannesburg, 2016

Declaration

I declare that this dissertation is my own, unaided work, except where otherwise acknowledged. It is being submitted for the degree of Masters of Science in Electrical Engineering to the University of the Witwatersrand, Johannesburg, South Africa. It has not been submitted before for any degree or examination at any other university.

Candidate Signature: .....

Name: .....

Date: (Day).....(Month).....(Year).....

Abstract

Power-line communications can be used for the transfer of data across electrical networks in applications such as automatic meter reading in smart grid technology. As the power-line channel is harsh and plagued with non-Gaussian noise, robust forward error correction schemes are required. This research is a comparative study where a Luby transform code is concatenated with power-line communication systems provided by an up-to-date standard published by électricité Réseau Distribution France named G3 PLC. Both decoding using Gaussian elimination and belief propagation are implemented to investigate and characterise their behaviour through computer simulations in MATLAB. Results show that a bit error rate performance improvement is achievable under non worst-case channel conditions using a Gaussian elimination decoder. An adaptive system is thus recommended which decodes using Gaussian elimination and which has the appropriate data rate. The added complexity can be well tolerated especially on the receiver side in automatic meter reading systems due to the network structure being built around a centralised agent which possesses more resources.

This dissertation is dedicated to my family and friends who have shown me great support over the years.

Acknowledgements

The author would firstly like to acknowledge his family for the constant emotional and monetary support provided throughout the course of his academic career which has led to the completion of this masters dissertation.

The author is also thankful for the guidance and supervision provided by Professor Ling Cheng as well as the facilities provided by the University of the Witwatersrand. Furthermore, the aid of Gareth Timm, Ellen de Mello Koch and Ryan Strange with proof reading of this dissertation is highly appreciated.

Acknowledgement must finally be provided to the Center for Telecommunications Access and Services (CeTAS) as well as the University of the Witwatersrand scholarship office which have given their financial support in the last two years in the guise of bursaries and merit awards.

Table of Contents

Declaration i

Abstract ii

Dedication iii

Acknowledgements iv

List of Figures viii

List of Tables x

List of Abbreviations xi

List of Symbols xiii

Chapter 1: Introduction 1

1.1 Problem Statement 3
1.2 Research Significance 3
1.3 Scope and Research Objectives 4
1.4 Dissertation Organisation 5
1.4.1 Literature Review (Chapter 2) 5
1.4.2 Research Methodology (Chapter 3) 6
1.4.3 Comparative Study of a Time Diversity Scheme Applied to G3 Systems for Narrowband Power-Line Communications (Chapter 4) 6
1.4.4 Conclusion (Chapter 5) 7

Chapter 2: Literature Review **8**

2.1 Narrowband PLC Regulations and Standards 8
2.1.1 EN 50065-1 8
2.1.2 Iberdrola PRIME 8
2.1.3 eRDF G3 9
2.1.4 IEEE 1901.2 10
2.2 PLC Channel Modelling 10
2.2.1 Signal Approach 11
2.2.2 Probabilistic Approach 14
2.3 Time Diversity Techniques 17
2.3.1 Interleaving 17
2.3.2 Repetition Codes 18
2.3.3 Fountain Codes 19
2.4 Telecommunication System Simulation 20
2.4.1 Hardware Implementation 20
2.4.2 Software Implementation 21

Chapter 3: Research Methodology **22**

3.1 Experimental Systems 22
3.1.1 G3 PLC Benchmark System 22
3.1.2 LT-modified G3 Systems 23
3.2 Forward Error Correction 23
3.2.1 LT Code 24
3.2.2 Reed-Solomon Code 28
3.2.3 Convolutional Code 30
3.2.4 Repetition Code 32
3.2.5 Interleaver 33
3.3 Channel Model 35
3.3.1 Background Noise 36
3.3.2 Impulse Noise 36
3.4 Digital Modulation 37
3.4.1 Single Carrier Modulation 37
3.4.2 Orthogonal Frequency-Division Multiplexing 38

Chapter 4: Comparative Study of a Time Diversity Scheme Applied to G3 Systems for Narrowband Power-Line Communications **42**

4.1 Current Industry Standard G3 Simulation Performance Analysis . 43

4.2 LT-Modified G3 System Performance Analysis 45
4.3 System Complexity Comparison 51
4.4 Conclusion from Simulation Results 52

Chapter 5: Conclusion **54**

5.1 Research Summary 54
5.2 Recommendations and Possible Future Work 55
5.3 Conclusion 55

References **57**

Appendix A: Derivation of Inverse CDF Sampling Formula for Exponential Distribution **64**

List of Figures

2.1 Gilbert-Elliott Markov chain channel model. 15

2.2 Fritchman Markov chain model. 16

2.3 Block interleaving with Λ value of 4 and n_{int} value of 4. a) Original binary sequence with 4 codewords. b) Interleaving array. c) Transmitted binary sequence with 4 interleaved codewords. 18

3.1 G3 PLC system block diagram. 22

3.2 LT-modified G3 PLC system. 23

3.3 Ideal Soliton Distribution with $k = 50$. 25

3.4 Robust Soliton Distribution with $k = 50$, $Q = 10$ and $\delta = 0.05$. 26

3.5 BP decoding procedure illustrated as a series of bipartite graphs. (a) y_1 identified as packet of degree 1. (b) x_1 recovered and removed from all packets y_j which contain it, y_2 identified as new packet of degree 1. (c) Decoding process terminated, all source packets recovered. 27

3.6 GE decoding procedure overview. (a) Received packets inserted into matrix. (b) A matrix is triangulated and (c) back-substitution is performed to obtain original source packets. 28

3.7 RS code shortening procedure. 30

3.8 Half-Rate convolutional encoder with L value of 7 and generator $\mathbf{g} = [171\ 133]$ in octal form. 31

3.9 G3 block interleaving example. a) Original binary data. b) Interleaved binary data. 35

3.10 BPSK constellation diagram. 37

3.11 DQPSK constellation diagram. 38

3.12 OFDM modulator block diagram. 39

3.13 OFDM demodulator block diagram. 39

4.1 BER vs E_b/N_0 for G3 system with 40 OFDM symbols and (21, 13) RS over PLC channel with varying impulse rate parameter. 43

4.2 BER vs E_b/N_0 for G3 system with 56 OFDM symbols and (30, 22) RS over PLC channel with varying impulse rate parameter. 44

4.3 BER vs E_b/N_0 for G3 system with 252 OFDM symbols and (141, 133) RS over PLC channel with varying impulse rate parameter. 44

4.4 Performance depending on code rate at various E_b/N_0 values for LT-modified G3 system with 252 OFDM symbols, (141, 133) RS code, λ value of 1/0.015 and a Q value of 50 using a BP decoder. 46

4.5 Performance depending on code rate at various E_b/N_0 values for LT-modified G3 system with 252 OFDM symbols, (141, 133) RS code, λ value of 1/0.015 and a Q value of 50 using a GE decoder. 46

4.6 Decoding probability based on LT code rate for LT-modified G3 system with 252 OFDM symbols, (141, 133) RS code, λ value of 1/0.015 and a Q value of 50 using a BP decoder. 47

4.7 Decoding probability based on LT code rate for LT-modified G3 system with 252 OFDM symbols, (141, 133) RS code, λ value of 1/0.015 and a Q value of 50 using a GE decoder. 47

4.8 BER vs E_b/N_0 for LT-modified systems with 40 OFDM symbols, (21, 13) RS and Q value of 10 over PLC channel with varying impulse rate parameter. 49

4.9 BER vs E_b/N_0 for LT-modified systems with 56 OFDM symbols, (30, 22) RS and Q value of 20 over PLC channel with varying impulse rate parameter. 49

4.10 BER vs E_b/N_0 for LT-modified systems with 252 OFDM symbols, (141, 133) RS and Q value of 50 over PLC channel with varying impulse rate parameter. 50

List of Tables

1 CENELEC frequency band division. 9

2 (4, 1) repetition code majority logic decoding rule. 34

3 G3 raised cosine window sample multipliers. 40

4 OFDM transceiver specifications summary. 41

5 G3 and LT-modified G3 performance comparison. 51

List of Abbreviations

AMR	**A**utomatic **M**eter **R**eading
ANSI	**A**merican **N**ational **S**tandards **I**nstitute
ARIB	**A**ssociation of **R**adio **I**ndustries and **B**usinesses
AWGN	**A**dditive **W**hite **G**aussian **N**oise
BER	**B**it **E**rror **R**ate
BN	**B**ackground **N**oise
BP	**B**elief **P**ropagation
BPSK	**B**inary **P**hase-**S**hift **K**eying
CC	**C**onvolutional **C**ode
CDF	**C**umulative **D**istribution **F**unction
CENELEC	**C**omité **E**uropéen de **N**ormalisation **ÉLEC**trotechnique
CSMA	**C**arrier **S**ense **M**ultiple **A**ccess
DBPSK	**D**ifferential **B**inary **P**hase-**S**hift **K**eying
DQPSK	**D**ifferential **Q**uadrature **P**hase-**S**hift **K**eying
EMC	**E**lectro-**M**agnetic **C**ompatibility
ETSI	**E**uropean **T**elecommunications **S**tandards **I**nstitute
eRDF	**é**lectricité **R**éseau **D**istribution **F**rance
FCC	**F**ederal **C**ommunications **C**ommission
FCH	**F**rame **C**ontrol **H**eader
FEC	**F**orward **E**rror **C**orrection
FER	**F**rame **E**rror **R**ate

FFT	**F**ast **F**ourier **T**ransform
FSK	**F**requency-**S**hift **K**eying
GE	**G**aussian **E**limination
IEC	**I**nternational **E**lectro-technical **C**ommission
IFFT	**I**nverse **F**ast **F**ourier **T**ransform
IMP	**I**terative **M**essage **P**assing
IN	**I**mpulse **N**oise
ISI	**I**nter-**S**ymbol **I**nterference
ITU	**I**nternational **T**elecommunication **U**nion
LDPC	**L**ow-**D**ensity **P**arity-**C**heck
LT	**L**uby **T**ransform
MAC	**M**edia **A**ccess **C**ontrol
MV	**M**edium **V**oltage
NBI	**N**arrow**B**and **I**nterference
OFDM	**O**rthogonal **F**requency **D**ivision **M**ultiplexing
PDF	**P**robability **D**ensity **F**unction
PHY	**PHY**sical layer
PLC	**P**ower **L**ine **C**ommunications
PRIME	**P**owerline **R**elated **I**ntelligent **M**etering **E**volution
PSD	**P**ower **S**pectral **D**ensity
PSK	**P**hase **S**hift **K**eying
QAM	**Q**uadrature **A**mplitude **M**odulation
QPSK	**Q**uadrature **P**hase **S**hift **K**eying
RC	**R**epetition **C**ode
RS	**R**eed **S**olomon
SER	**S**ymbol **E**rror **R**ate
SNR	**S**ignal to **N**oise **R**atio
USRP	**U**niversal **S**oftware **R**adio **P**eripheral

List of Symbols

Symbol	Units	Description
A	–	Amplitude.
$a_0,\ a_1$	–	Attenuation parameters of a multipath channel model.
C	–	Impulse index of the Middleton impulse noise model.
c_0	meter per second	Speed of light.
D_i	meter	Distance travelled on i^{th} signal path path.
d	packet	Degree during LT encoding process.
d_{free}	-	Free distance of the convolutional code.
E_b	joule	Energy per information bit.
E_s	joule	Energy per symbol.
f	hertz	Frequency.
f_s	hertz	Sampling frequency.
g	-	Gain parameter.
k	packets	Number of source packets for the LT code.
k_{CC}	bits	Message size of convolutional code.
k_{RS}	bits	Message size of Reed-Solomon code.
k_{short}	bits	Message size of shortened Reed-Solomon codes.
L	–	Constraint length of the convolutional encoder.
l	bits	Length of the LT packets.
M	–	Modulation order.
m	–	Galois Field order.

N	path	Number of paths in a multipath channel model.
N_{cp}	samples	Number of cyclic prefix samples used in the OFDM transceiver.
N_{fft}	points	Number of FFT points used in the OFDM transceiver.
N_o	watt per hertz	Noise power spectral density.
N_{sc}	subcarriers	Number of subcarriers used in the OFDM transceiver.
N_{sym}	symbols	Number of OFDM symbols per G3 frame.
N_{total}	bits	Total number of bits per G3 frame.
N_{win}	samples	Number of samples used in the windowing of the OFDM symbols.
n	packets	Number of encoded packets from the LT code.
n_{CC}	bits	Codeword size of convolutional code.
n_{int}	bits	Number of bits in each interleaved codeword.
n_{rep}	bits	Codeword size of repetition code.
n_{RS}	symbols	Codeword size of Reed-Solomon code.
n_{short}	symbols	Codeword size of shortened Reed-Solomon code.
p_b	–	Probability of bit error.
p_e	–	Probability of error.
p_{gb}	–	Probability of transition from good to bad state.
p_{bg}	–	Probability of transition from bad to good state.
p_s	–	Probability of symbol error.
Q	–	Value of second spike of Robust soliton distribution.
R	–	Code rate.
$R_{effective}$	–	Effective code rate.
r	–	Size of un-padded bit stream input to the convolutional encoder.
S_i	symbol	Number of modulated symbols.
SNR	dB	Signal-to-noise ratio.
t	errors	Error correcting capability of error correcting code.
z	-	Exponent of attenuation factor in multipath channel model.
δ	–	Robust Soliton Distribution parameter.
ϵ	farad per meter	Dielectric constant.

θ	degree	Phase angle.
λ	–	Exponential distribution rate parameter.
Λ	–	Interleaving depth.
σ_i^2	–	Variance of impulse noise amplitude.
σ_{noise}^2	–	Variance of background noise amplitude.
τ	second	Delay of a path in a multipath channel model.

Chapter 1: Introduction

Power-line communications (PLC) is a technique which involves the implementation of a communication system over existing electrical supply installations [1]. These PLC systems are cost effective as a new architecture does not need to be installed for the communication medium and they can be utilised worldwide.

Two types of PLC categories generally exist namely broadband PLC operating at frequencies greater than 500 kHz and narrowband PLC operating at frequencies lower than or equal to 500 kHz. Narrowband PLC finds its uses in communications over long ranges with lower data rates and is therefore useful for applications involving both the monitoring and control of electrical systems [2]. On the monitoring side, as the demand for smart power management increases, techniques such as automatic meter reading (AMR) have been developed and are being actively researched to provide an efficient smart grid backbone [3–6]. An example of an application on the control side includes smart distribution grids over the medium voltage network where narrowband PLC can be responsible for the communications and the control of different devices such as switching certain systems on or off for the purpose of energy saving [7].

In an attempt to universalise narrowband PLC implementations, several standards have been developed. It can be observed that these standards tend to be very similar to the standards used in wireless systems. As an example, both the électricité Réseau Distribution France (eRDF) G3 PLC [8] and wifi 802.16-2004 standards [9] possess the same forward error correction (FEC) chain. As both communication channels are different (air interface versus power-lines) and possess different characteristics, it could possibly lead to inefficient systems. This is thus the motivation behind trying new schemes over the PLC channel such as presented in this research.

Forward error correction techniques fitting the category of time diversity can be used to protect the communication system over power lines from burst errors [10, 11]. Examples include using repetition codes (RC) which are of low implementation complexity or more complex schemes such as fountain codes. This research is focussed on rateless fountain codes named Luby transform (LT) codes which can generate any number of packets n from k input packets [12]. In the context of broadband PLC applications such as the distribution of high quality video, LT codes can provide an increase in performance [13, 14]. Further development in fountain codes resulted in the creation of raptor codes which provides a further increase in performance by precoding the input data with a high rate low-density parity-check (LDPC) code allowing both the encoding and decoding operations to be performed in linear time [15]. By using the LDPC code as an inner code as opposed to an outer code such as in raptor codes, performance can be increased further over the PLC channel [16]. This improvement stems from properties of LDPC codes which can be used to pinpoint packets that have been received in error and therefore discard them resulting in a lower chance of errors propagating during the decoding process. As faulty packets get dropped, the LT code then operates on a channel which acts as an approximation to an erasure channel.

Further research on this topic can be performed with regards to applying LT codes to systems provided by current day standards such as G3 PLC systems [8]. G3 PLC systems can be used for the communication requirements of AMR in smart grid applications. As G3 smart meter systems are already implemented in several areas [17, 18], an advantage is that the task of performing the modification on live systems is more practical should it prove to be beneficial. Secondly, in G3 systems, inner codes are short especially when compared to LDPC codes which require much larger codes for a significant increase in performance. Smaller packets therefore have increased protection which means that a smaller amount of data can get corrupted when a burst type error occurs.

1.1 Problem Statement

Narrowband communications in the lower frequency range is difficult due to the high level of noise in the PLC channel. From the literature, it has been stipulated that PLC systems could be improved through the use of time diversity techniques such as fountain coding and specifically LT codes. The problem is thus to investigate the performance of LT codes when concatenated with systems provided by up-to-date standards and determine what the complexity trade-off is.

The main research question answered within this dissertation can be stated as follows: *"Can systems provided by current narrowband PLC standards be made more robust through the use of fountain codes, specifically LT codes, such that a new system operates at a similar or better bit error rate value and how does this modification affect the complexity of the system?"*

1.2 Research Significance

Topics in the field of narrowband PLC technology are expected to develop further in the coming years with the advancement and need for smart grid applications such as power distribution and management [19]. This is especially true in developing countries where both the generation of power and installation of new communication system infrastructures in rural areas can be problematic such as in South Africa. If new PLC products need to be created for such scenarios the research that has been performed around various topics involving PLC can be used.

A further motivation and contribution of this research is that as G3 systems already exist in the field [17, 18], it would be more practical to perform this modification on live systems should the modification prove to be beneficial. Since the new modified systems must adhere to constraints specified in the standard and only involves the addition of a new concatenated section, it also means that it results in systems which are backwards compatible and therefore more applicable in various situations.

Finally, a component that makes this research significant is the fact that this new FEC scheme is original to the best knowledge of the author as no publications analysing

this specific communication system layout over the PLC channel have been published. The set-up recommendations provided based on the obtained results can be used for further research into LT-modified G3 systems which could eventually lead into the development of new and updated standards.

1.3 Scope and Research Objectives

This research focuses on improving communications over the PLC channel which can be used in the communication aspect of systems related to power delivery. A new original system is investigated in an attempt to improve the performance of PLC systems provided by an up-to-date standard called the G3 PLC standard [8]. This technology therefore meets the requirements for the communication section in the AMR component of smart grid applications.

In the first objective of the research, a link between the values of the fountain code parameters and the system performance is analysed. Knowledge of this relationship then allows PLC system designers to optimise the design according to different system specification requirements and channel situations or allow for the creation of an adaptive fountain coding scheme if channel estimation is available to the transceiver. Firstly, the encoder in the code encodes data packets according to the number of input packets available to the system as well as a probabilistic distribution named the robust Soliton distribution which possesses parameters that affect the behaviour of the system. Secondly, once these parameters are selected, the number of encoded packets sent by the encoder which determines the code rate must be selected as the system operates with a frame size limitation as discussed in chapter 4.

In the second objective of the research, the knowledge gathered in the first objective is applied as a proof of concept to assess the performance of the new systems. For an in depth analysis, two sets of systems using the same PLC channel model are implemented in a software environment to run simulations for the gathering of data required for the research. The first set of systems used as benchmark systems are programmed according to the specifications provided in one of the currently existing narrowband PLC standards (G3 PLC) and covers the range of systems from best to worst-case set-

ups. This thus allows for the research results to be applicable within the narrowband PLC industry. The second set of systems which are implemented are modified versions of the same previous systems but which makes use of a different time diversity technique called fountain coding. Specifically, G3 systems are concatenated with an LT code which is used as an outer code instead of the specified RC. These systems are all tested with several channel conditions which also cover the range of noise parameters which are typically to be expected in real life PLC applications. The simulation of these systems operating over the PLC channel allows for the gathering of data such as bit error rate (BER) performances as well as the value of message overhead (fountain code rate) required for decoding during each iteration. This data is then used to determine any trade-offs which can exist between the encoding/decoding complexity of the systems and both the error rate performances and overall data rates.

Enough information is provided for the knowledgeable reader to fully understand all components of the research. Further data from testing as well as arguments are provided to explain the obtained results as well as how they could possibly lead to future research and be improved.

1.4 Dissertation Organisation

An overview of this masters dissertation is provided within this section in order for the reader to have a clear idea of what to expect and thus gain a better understanding of the research.

1.4.1 Literature Review (Chapter 2)

This chapter presents the information that has been discovered during the literature review component at the start of the research. This information allows the research to be contextualised and presents the work that has been done in the field up to the point of writing of this document. This includes topics about research that has been previously completed and which can be related to this topic. The first theme covered includes several current day narrowband PLC standards provided by various professional institutions and which have been adopted internationally. The second theme covered includes the PLC channel modelling and the methods that have been used to achieve a

model which is accurate for the purpose of computer simulations. In the third theme different time diversity techniques are explored focussing on the research that has been done when they are applied to the field of PLC, especially when including the use of fountain coding. The final theme discusses various software that can be used for the purpose of simulating a telecommunication system in a personal computer environment.

1.4.2 Research Methodology (Chapter 3)

The research methodology is presented which describes the three major components of the research that are implemented in software i.e. the chosen channel model parameters, the benchmark systems transceiver layout and the LT-modified systems transceiver layout. This includes an in depth explanation into the way in which the LT code encoder and decoder operate as well as the various other components present in the system including a Reed-Solomon (RS) encoder/decoder, a convolutional code (CC) encoder/decoder, an interleaver, a repetition code encoder/decoder and the orthogonal frequency-division multiplexing (OFDM) transmitter/receiver with associated modulation schemes.

1.4.3 Comparative Study of a Time Diversity Scheme Applied to G3 Systems for Narrowband Power-Line Communications (Chapter 4)

The results of the paper covering this topic which has been submitted to the *IEEE Transactions on Consumer Electronics* is shown in this chapter. The simulation results are presented and analysed which allow for the successful completion of the objectives listed in Section 1.3 and thus answer the research question. Firstly, simulations are performed for a range of benchmark systems operating under various channel conditions to obtain an idea of how current day systems are able to perform on the PLC channel. Secondly, a method for an LT codec design is presented and implemented which allows for the simulation of the performance of LT-modified systems under the same conditions as that of the previous tests, allowing for a fair comparison. In this chapter a complexity analysis is also given which shows that the increase in complexity added by the addition of the LT code can be well tolerated in applications where it would be used such as AMR in smart grids.

1.4.4 Conclusion (Chapter 5)

A conclusion is drawn which summarises and wraps up the findings of this research in the final chapter. This includes recommendations and possible future work which could be further explored in future research.

Chapter 2: Literature Review

2.1 Narrowband PLC Regulations and Standards

Several standards have been created by various associations in an attempt to standardise the implementation of narrowband PLC systems with frequencies lower than 500 kHz. These standards typically define both the physical (PHY) and media access control (MAC) layer protocols as well as the electromagnetic compatibility and regulations for coexistence with other systems. The main up to date standards used in the narrowband PLC industry are introduced below.

2.1.1 EN 50065-1

The Comité Européen de Normalisation Électrotechnique (CENELEC) released a standard first published in 2001 specifying the allowable transmitter signal power in the 3 kHz to 148.5 kHz narrowband frequency range [20]. The power limit is usually in the range of 120 dB μV in an attempt to prevent electromagnetic interference with other systems. This limit can be considered low, resulting in challenges for communication system implementations. This standard splits this frequency range into the four bands shown in Table 1.

The CENELEC A band lends itself to be the most appropriate band for the implementation of smart grid narrowband PLC services and is thus the one utilised in most narrowband PLC standards.

2.1.2 Iberdrola PRIME

The **P**owe**R**line **I**ntelligent **M**etering **E**volution (PRIME) alliance project from Iberdrola developed their standard for interoperability of smart grid applications over the power grid on the CENELEC A band since the year 2007 [21]. This specification

Table 1: CENELEC frequency band division.

Band	Frequency Range (kHz)	Band Utilisation
A	9-95	Energy monitoring/controlling
B	95-125	Consumer channel
C	125-140	Consumer channel, requires the use of CSMA
D	140-148.5	Consumer channel

attempts to achieve high data rates over low voltage networks. The specification of interest is the PHY layer specification which specifies the modulation scheme as using orthogonal frequency division multiplexing (OFDM) defined in the ITU-T G.9904 standard [22] in combination with m-ary differential phase-shift keying schemes (DBPSK, DQPSK and D8PSK). PRIME systems make use of the 42 kHz to 89 kHz range in the CENELEC bands and can use frequencies in the 10 kHz to 490 kHz range if it is used in the frequency bands defined by the Federal Communications Commission (FCC) in the USA or 10 kHz to 450 kHz range in Japan where the bands are governed by the Japan Association of Radio Industries and Businesses (ARIB) [23]. The FEC scheme is defined as using a half-rate convolutional encoder with repetition code, scrambler and bit interleaving.

2.1.3 eRDF G3

Électricité Réseau Distribution France (eRDF) developed their own standard in 2011 which is very similar to the PRIME standard involving smart grid services. The G3 systems are also implemented on the CENELEC A, FCC and ARIB bands but they target lower data rates on the medium voltage network with increased robustness. This standard specifies an OFDM based communication scheme which can use either BPSK, DBPSK or DQPSK depending on the channel conditions and the channel rate required. The frequency range used is from 36 kHz to 91 kHz. G3 systems use the same FEC

chain as the PRIME standard but with an added Reed-Solomon (RS) code as an outer code increasing its performance for a trade-off in increased system complexity.

2.1.4 IEEE 1901.2

The IEEE 1901.2 standard gives the specification for devices operating at frequencies less than 490 kHz [24]. It is OFDM based and meant to be compatible with both the G3 PLC and PRIME standards when used in the CENELEC A band. The modulation schemes supported are DBPSK, DQPSK, D8PSK, BPSK, QPSK, 8PSK and 16-QAM. The forward error correction used is identical to its G3 counterpart with the use of an 8 or 16 byte parity RS outer code with a convolutional inner code, 4 or 6 times repeater, time and frequency interleaver as well as a scrambler. Furthermore, this standard also makes use of adaptive tone mapping which selects the sub-carriers to be used in the communication depending on the currently estimated channel characteristics.

2.2 PLC Channel Modelling

In this section the literature concerned with accurate PLC channel modelling in a software environment is reviewed. Since the power line channel is shared amongst many electrical systems it is known to be very harsh. Research has thus been conducted to try and characterise it [25, 26]. From measurements taken in various settings it has been found that the dominant types of noise present are classified as background noise (BN), narrowband interference (NBI) as well as impulse noise (IN) [27]. The combination of these types of interference result in a non-Gaussian channel which exhibits bursty characteristics where a burst error is considered to be a sequence of bits or symbols that get received in error. For example, in (1), a burst of length 4 is observed in the received binary sequence considering that 13 consecutive 0's were sent over the channel.

$$\mathbf{r} = [0001011000000] \tag{1}$$

This is due in part to the allowable transmitting power being quite low (120-134 dB (µV)) [20] with respect to the impulsive noise and narrowband interference components which take over the signal when they occur. During this time, the channel can be considered to be unusable where even standard FEC techniques may not be enough for successful recovery of the data as the received packets get completely corrupted.

Generally, two different approaches can be employed to model the PLC channel. The first is a signal approach where the additive noise signals are simulated and added to the transmitted signal. The second is a probabilistic approach which usually makes use of stochastic models such as Markov chain models characterising the channel with different states. Both of these approaches are described next.

2.2.1 Signal Approach

Background noise: The source of this type of noise can be attributed to environmental factors and thermal noise from the front-end amplifiers of the receiver as in most communication systems. BN is usually more severe on the MV channel than on the low voltage channel [28]. It is usually coloured on the PLC channel but is often assumed to be modelled as additive white gaussian noise (AWGN). As such, this noise can be modelled by the following procedure [29]. The noise generated is dependent on the signal to noise ratio (SNR) selected by first determining the noise power spectral density N_o as shown

$$N_o = E_b \times 10^{\frac{-SNR_{dB}}{10}} \tag{2}$$

where E_b is the energy per information bit. The average noise power can then be determined from

$$\sigma^2_{noise} = \frac{N_o \times f_s}{2} \tag{3}$$

where f_s is the sampling frequency. The noise to be added at every sample point of the signal is then obtained by

$$n(kT) = \sqrt{\sigma^2_{noise}} \times u \tag{4}$$

where u is a normally distributed random number of mean zero, variance one and standard deviation of one. It should be noted that for a channel which is only affected by AWGN, the simulation should be run until a minimum of 100 errors have occurred for statistical significance. When channels can be considered as AWGN channels, closed form formulas can be used for the analysis of most communication systems over it. For example, in the case of DBPSK and DQPSK, the bit error rates (BER) can be analysed

according to the two following formulas respectively [30]

$$p_s = p_b = 2Q\left(\sqrt{\frac{2E_b}{N_o}}\right) - 2Q^2\left(\sqrt{\frac{2E_b}{N_o}}\right) \tag{5}$$

$$\begin{aligned} p_s = 4Q\left(\sqrt{\frac{2E_b}{N_o}}\right) - 8Q^2\left(\sqrt{\frac{2E_b}{N_o}}\right) \\ + 8Q^3\left(\sqrt{\frac{2E_b}{N_o}}\right) - 4Q^4\left(\sqrt{\frac{2E_b}{N_o}}\right) \end{aligned} \tag{6}$$

where p_s represents the probability of symbol error, p_b the probability of bit error, E_b the energy per bit, N_o is the noise power spectral density and $Q(x)$ is the Q function as defined

$$Q(x) = \frac{1}{\sqrt{2\pi}} \int_x^{\inf} e^{\frac{-t^2}{2}} dt. \tag{7}$$

It should be noted that due to the non-Gaussian noises presented next, that these formulas may not be used for the overall performance over the PLC channel and that in this case no readily made formula is available for simple analysis.

Narrowband interference: Signals from wireless transmission can leach into the PLC channel resulting in NBI [31]. One of the causes resulting in this type of signal leakage arises when the electrical conductors used in the communication system act as antennas which can pick up ambient signals. This type of noise can be emulated by generating modulated sinusoidal noise with a varying central frequency [32]. The frequencies of these components are typically dictated by central radio broadcasting stations and television screening frequencies or by their harmonics. This can be represented mathematically by a slightly modified version of the equation described in [33]

$$s_{NBI}(t) = \sum_{i=1}^{N} A_i(t)\sin(2\pi f_i + \theta_i)\mathrm{imp}\left(\frac{t - t_{arr,i}}{t_{w,i}}\right) \tag{8}$$

where the N NBI waveforms are defined by five parameters, namely the NBI amplitudes $A_i(t)$, the NBI centre frequencies f_i, the NBI phases θ_i, the NBI arrival times $t_{arr,i}$ and the NBI durations $t_{w,i}$. It should also be noted that $\mathrm{imp}(t)$ is a generalised impulse

function which has an amplitude value of one and a width of one.

Impulse noise: Noise appearing in the form of impulses appear both synchronously and asynchronously to the mains voltage as well as at apparently random timings in the power line channel. The impulses found to be synchronous with the mains can be attributed to circuit components such as silicon-controlled rectifiers [25]. In the case of impulse noises asynchronous with the mains, switching regulators can be found to be a possible cause. Finally, random impulses occur due to human interactions with the electrical network when elements such as light switches or thermostats get switched on. This type of noise can be represented mathematically as [33]

$$s_{IN}(t) = \sum_i A_i \ \mathrm{imp}\left(\frac{t - t_{arr,i}}{t_{w,i}}\right) \tag{9}$$

where the three parameters used to define the impulse noises are the amplitudes A_i, the impulse durations (width) $t_{w,i}$, the impulse arrival times $t_{arr,i}$ and the impulse function $\mathrm{imp}(t)$ as previously defined. The inter-arrival rate (time between impulses) and thus the arrival rate can be modelled as a random variable generated from the inverse transform sampling of a Poisson Process exponential cumulative distribution function (CDF)

$$F(t) = 1 - e^{\lambda t} \tag{10}$$

where λ is the rate parameter determining how often an impulse occurs. An alternative approach for impulse noise modelling in the PLC environment is through the use of the Middleton Class-A model [34–36]. This model is defined by the probability density function (PDF)

$$p(n) = \sum_{j=0}^{\infty} P_j \frac{1}{\sqrt{2\pi\sigma_j^2}} e^{-\frac{n^2}{2\sigma_j^2}} \tag{11}$$

where P_j and σ_j^2 are defined as:

$$P_j = \frac{e^{-C} C^j}{j!} \tag{12}$$

$$\sigma_j^2 = \sigma_i^2 \frac{j}{C} + \sigma_{noise}^2 \tag{13}$$

where the parameter C is defined as the impulsive index and controls the severity of the impulses, σ_i^2 is the IN variance and σ_{noise}^2 is the Gaussian noise variance. The amplitude of impulses in the PLC channel are found to have a maximum value of 50 dB above the BN floor [25]. The width of the impulses which affects how many symbols get corrupted by each impulse is found to be uniformly distributed in the range of 10 μs to 1 ms [37].

Multipath Model: Due to the topology of the PLC channel, multipath signal propagation and signal attenuation further degrades the transmitted signal [38]. The multipath propagation is due to the possibility of there being any number of cable paths branching off the main path from the transmitter to the receiver. Wave reflections thus occur when the signal travels between mediums with different characteristic impedances. A model of the channel transfer function which has been developed is defined by [38]

$$\underline{H}(f) = \sum_{i=1}^{N} g_i \cdot e^{-(a_0 + a_1 f^z) D_i} \cdot e^{-j2\pi f \tau_i} \tag{14}$$

where N is the number of paths, g_i is the weighting factor of every individual path, a_0 and a_1 are attenuation parameters, D_i is the distance of every individual path and z is the exponent factor coefficient. The variable τ_i is the delay of each path determined by the function

$$\tau_i = \frac{D_i \sqrt{\epsilon_r}}{c_0} \tag{15}$$

where ϵ is the dielectric constant of the insulating material and c_0 is the speed of light. A problem with the provided parameter values is that they only apply to the frequency range from 500 kHz to 20 MHz which is above that of the one used by G3 systems. For this model to be used, new channel measurements would therefore be needed for a good simulation accuracy. On the other hand, G3 systems also perform equalisation and it is thus assumed that filter characteristics of the channel are effectively cancelled out removing the need for a multipath model in the system.

2.2.2 Probabilistic Approach

As opposed to the signal approach which involves creating additive noise signals which are added to the transmitted signal, the probabilistic approach involves generat-

ing a binary error vector which can be XOR'ed with the binary vector to be transmitted. These types of model can therefore act directly on a binary stream and operate at a higher level by combining the channel as well as the modulator and demodulator into a single module.

Gilbert-Elliott Model

To model bursty channels, partitioned Markov chains such as the Gilbert-Elliott model may be used [39, 40]. This technique describes the system using both a good state and a bad state that introduce memory to the system which can then characterise burst errors. The model is defined by its state transition probability matrix and probability of transmission error within both states. p_{gb} is defined as the transition probability of going from the good state to the bad state and p_{bg} is the transition probability of going from the bad state to the good state. Typically it is assumed that no or few errors occur within the good state, i.e. the probability of error $p_e = 0$ and that worse channel characteristics such as a probability of error $p_e = 0.5$ occur in the bad state. The graphical representation of this model can be seen in Figure 2.1.

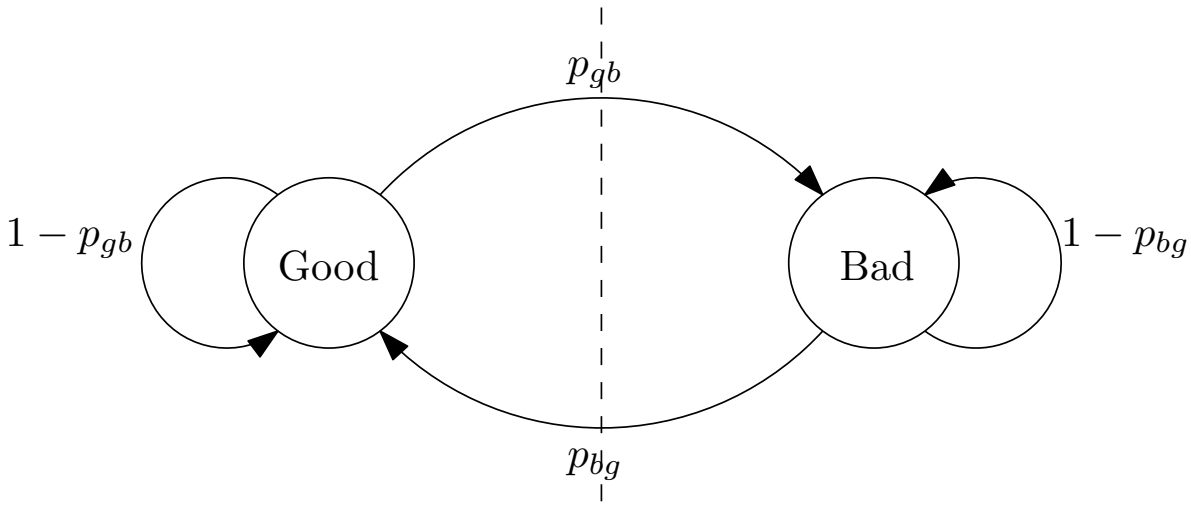


Figure 2.1: Gilbert-Elliott Markov chain channel model.

Fritchman Model

From the literature it is seen that a more precise partitioned Markov chain model named the Fritchman model [41] can be used to model bursty channels. The Fritchman model is obtained by including more than two different states and partitioning them into K good and N-K bad states as shown in Figure 2.2.

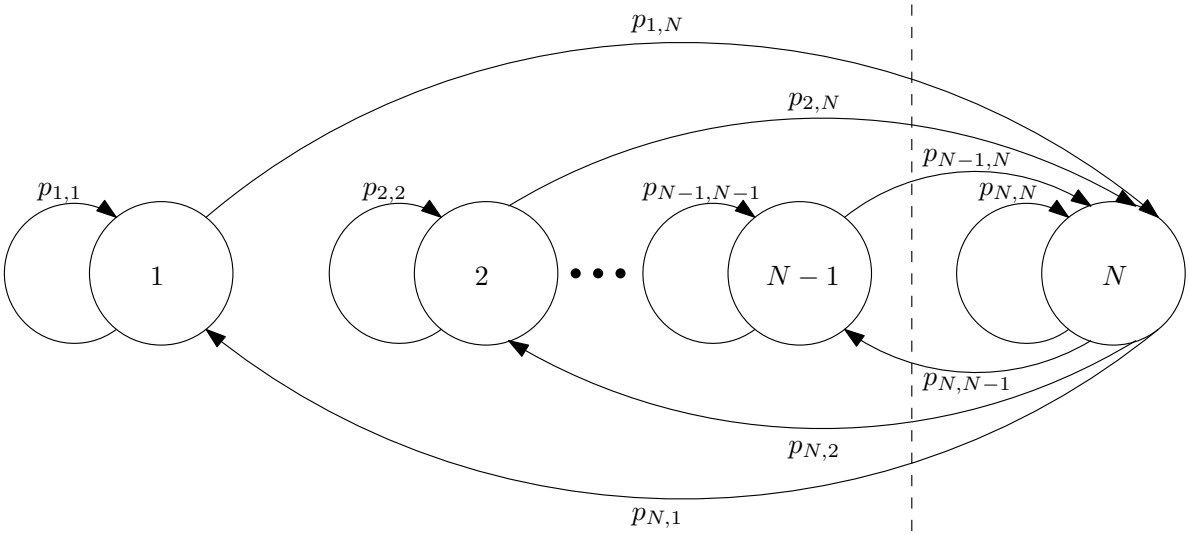


Figure 2.2: Fritchman Markov chain model.

Different model orders can then be generated where the order signifies how many preceding states influence the current state. These Markov models are then fully defined by three parameters: the state transition probability matrix, the initial state probability matrix and the output symbol probability matrix. A method was developed to find the parameters required for the definition of both a first and second order Fritchman model applied to a PLC channel [42]. To accomplish this, a physical communication system must be implemented and used either over existing power lines or a test bed which approximates it. To implement this physical system, software defined radios such as Universal Software Radio Peripherals (USRP) can be used to obtain and measure data. The state transition probabilities are then obtained by using the Baum-Welch algorithm on the error sequence obtained from those measurements.

Using any of these two previously stated probabilistic methods to generate an error sequence has the advantage of accelerating the simulation speed and acquiring results

faster. This is due in part to the number of binary data being smaller than the number of time signal sampling points as well as the fact that the XOR operation required to combine the transmitted binary sequence and error binary sequence can be performed quicker than signal processing which might be needed when simulating at the signal level. On the other hand, the major drawback with these methods is that different values for the error probabilities and state transition probabilities are required for every SNR values which are to be simulated. As stated previously, the statistical values of the Markov models can be obtained from data obtained from physical measurements. This is a lengthy process and is outside the scope of this research, therefore a signal level simulation approach will be used in this research.

2.3 Time Diversity Techniques

Time diversity schemes offer a reliable way of combating the packet loss problem inherent to the non-Gaussian PLC channel in broadband power-line communications with reduced encoding/decoding time and complexity [13, 14]. This idea has been explored further by applying it in the context of narrowband power-line communications [10, 11]. Furthermore it has been shown that fountain codes are an efficient method for combating burst errors by treating faulty packets as erasures [16]. Time diversity includes techniques such as interleaving, rateless erasure codes named fountain codes and repetition codes.

2.3.1 Interleaving

Bit interleaving is a technique which involves breaking down several codewords and mixing them up such that several parts of a codeword are spread through time. The codewords then get re-assembled once they arrive at the receiver. Interleaving techniques can generally be split into two broad categories: deterministic interleaving (such as block interleaver, Berrou-Glavieux interleaver, etc) and random interleaving (such as pseudo-random interleavers, semi-random interleavers, etc). Two types of interleaving techniques commonly used are block interleaving and convolutional interleaving. Block interleaving requires the storage of several codewords into an array with Λ rows and n_{int} columns representing the number of bits in each codeword. The data then gets read out in a different order. This thus results in burst errors being spread across Λ different

codewords where Λ is defined as the interleaving depth. This procedure is shown in Figure 2.3 with a Λ value of 4 and n_{int} of 4.

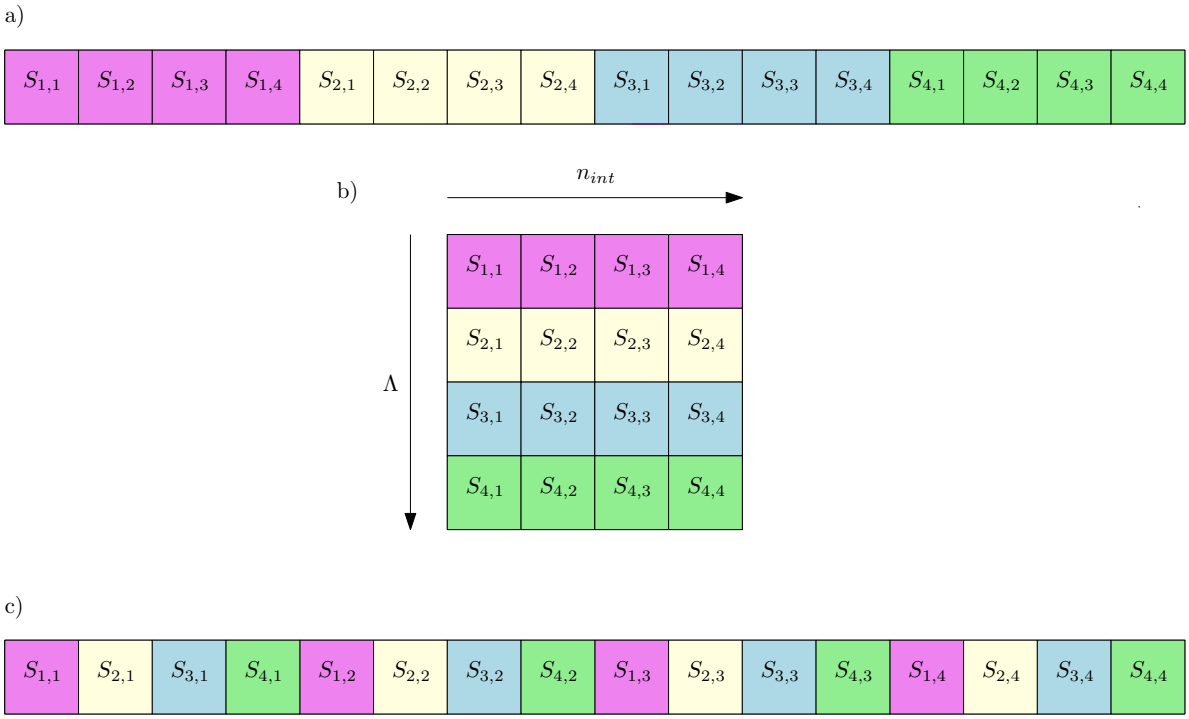


Figure 2.3: Block interleaving with Λ value of 4 and n_{int} value of 4. a) Original binary sequence with 4 codewords. b) Interleaving array. c) Transmitted binary sequence with 4 interleaved codewords.

Convolutional interleaving on the other hand involves multiplexing a codeword onto different branches which contain a varying number of shift registers. Both methods introduce considerable latency to the system due to the use of a buffer and the fact that the memory must first be filled before being read out at both the transmitter and receiver.

2.3.2 Repetition Codes

RCs function by repeating every codeword input to the encoder a certain amount of times such that each repeated codeword is usually affected differently by the channel (since they travel through the channel at different times). The advantage of an RC is that both the encoder and decoder are simple to implement and require few logic components, however they usually require a rate less than or equal to $\frac{1}{3}$. The decoding

can be performed by a majority logic decoder where the bit that occurs the most at a certain location in all the repeated codewords is selected as the transmitted binary digit. In the case of a tie, a bit can be selected at random or the position can be taken as an erasure. It should be noted that RC provides no performance increase over channels affected by AWGN only and actually performs worse as the repetition factor increases [43]. The strength of this code is therefore against impulse noise which may affect only a subset of the repetitions.

In the context of narrowband PLC, it is shown that a communication system can be well protected by the addition of an RC in a coding scheme [11]. In this case, an RC is concatenated with a permutation code using M-ary frequency-shift keying (FSK) allowing for the detection of IN and NBI. The advantage of this scheme is that a good performance is achieved with a low increase in complexity considering that RCs can be decoded using majority logic decoding. For a further increase in performance it is advised that an additional outer code may be used. It is interesting to note that the G3 standard uses a similar set-up in robust mode with an RC concatenated with two different outer codes (RS and CC code).

2.3.3 Fountain Codes

Fountain codes are rateless codes that are typically used with packets at the network layer over erasure channels. They are characterised by the term rateless due to the fact that they can generate any number of encoded packets n for a set of source packets k. They function by allowing the recovery of the k original packets when the receiver correctly receives a certain number of packets usually only slightly larger than k.

Luby Transform Code: Luby Transform (LT) codes operate by sending a stream of packets generated by the XOR operation performed on d packets randomly selected from the original packets list [12]. The integer value d is generated from a discrete distribution which is typically the robust Soliton distribution derived from the ideal Soliton distribution. Several parameters of this distribution can be optimised depending on what is required in the system.

Raptor Code: Raptor codes are a type of fountain code which differ from LT codes in the sense that the packets are pre-coded (typically by an LDPC code) before being put into an LT encoder [15]. Due to the pre-coding section, they are more efficient than LT codes since they can be both encoded and decoded in linear time, however the trade-off is that an increase in circuit logic complexity is required. The most common raptor code implementations encountered are the RaptorQ code [44] and its predecessor, the Raptor 10 code [45].

The strength of fountain codes in PLC applications is that when a packet gets corrupted by impulse noise, the information it contains can be recovered by being redundantly contained in other packets that get successfully recovered. A scheme using a fountain code has been successfully shown to work when it is used as an outer code in combination with permutation coding [10]. A further advantage is that fountain codes can achieve better data rates when compared to repetition codes. Further proof is available which shows considerable increase in performance over channels affected by IN [13, 14, 16]. The best performance is achieved when an LT code is used as an outer code whilst an LDPC code is used as an inner code (raptor code with the code order flipped). A question which might arise from these results is whether fountain codes are also applicable to channels that also get affected by AWGN as this is not explicitly covered in the surveyed literature.

2.4 Telecommunication System Simulation

To gather the data needed to successfully answer the research question, the simulation of PLC telecommunication systems must be implemented either in a software or hardware environment. Advantages and disadvantages exist to both methods which are discussed below.

2.4.1 Hardware Implementation

Physical PLC system simulations can be implemented through the use of hardware such as USRPs or Arduino boards using the Mamba Narrowband PLC shield [46, 47]. In the case of PLC systems, a communication channel test bed must also be built such that the receiver and transmitter may be connected to it and communicate. This

test bed must be built with electrical wires which can take on various different network topologies and must have various electrical apparatuses connected to it. These electrical apparatuses are required to attempt and produce interference which would normally be encountered on a real PLC channel. As the implementation of a physical system is beyond the scope of this research, a software implementation approach for simulation purposes is instead chosen.

2.4.2 Software Implementation

Implementing a telecommunication system in software requires the coding of many individual parts which are then combined to create the whole system. For example, the components of the transmitter, receiver and channel can separately be implemented and then connected together. This can be achieved using programming language such as C or C++ but can also be implemented with scripting languages such as MATLAB or GNU Octave. The advantage of using MATLAB is that it possesses various toolboxes such as the signal processing toolbox and the communications systems toolbox [48, 49]. These toolboxes contain pre-made functions which can be used in this research and therefore accelerate its completion. Due to these advantages MATLAB is chosen as the implementation tool for this research. The disadvantage that should be noted is that simulation times will be greater when compared to C or C++ implementations as the functions operate at a higher level of abstraction.

Chapter 3: Research Methodology

This chapter describes the research background required for understanding the research. The individual components of every system used in the research are therefore described here.

3.1 Experimental Systems

3.1.1 G3 PLC Benchmark System

The base system used for performance comparison is the communication system stipulated in the G3 standard which can be seen in block diagram form in Figure 3.1.

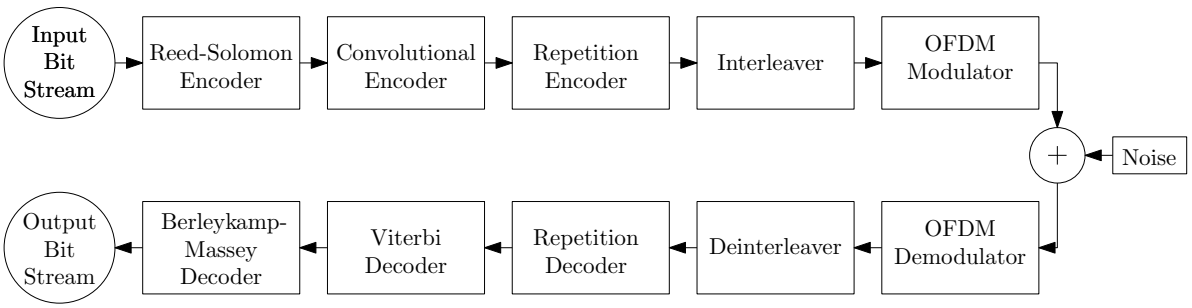


Figure 3.1: G3 PLC system block diagram.

The motivation behind this choice is the focus on FEC within this research and that according to simulation results, it is deemed that G3 systems contain a stronger and more complex FEC section than their PRIME counterparts due to the extra RS code layer [50]. It should be noted that the transmitter and encoder sections are well defined in the standards but that the receiver and decoder implementations are not therefore leaving the implementation decision to the author. As can be seen in Figure 3.1, this system is composed of a concatenated scheme containing an RS code followed by a CC, RC and interleaver being fed into an OFDM transmission system. G3 systems can

operate in two different modes: normal mode and robust mode. The RC is only active in robust mode and is thus this is the mode selected for this research. The transmitted signal then goes through a PLC channel which is affected by different additive noises.

3.1.2 LT-modified G3 Systems

In the prototype systems used as a proof of concept, the repetition code from the G3 system is replaced by an LT code which is concatenated with the FEC chain. The RS and CC encoder as well as the interleaver are maintained in the design as it allows for the correction of random errors and can provide information to the outer LT code [16]. This configuration therefore has the effect of allowing the LT code to operate under conditions approximating a binary erasure symmetric channel by dropping corrupted packets in instances where errors can successfully be detected. To make the system comparisons fair, these inner codes as well as their associated rates are kept constant between the G3 and LT-modified G3 systems. On top of this, the RS code provides feedback as to which received packets are correctly decoded or which are still faulty and thus should be avoided by the LT decoder. Figure 3.2 shows the new modified system.

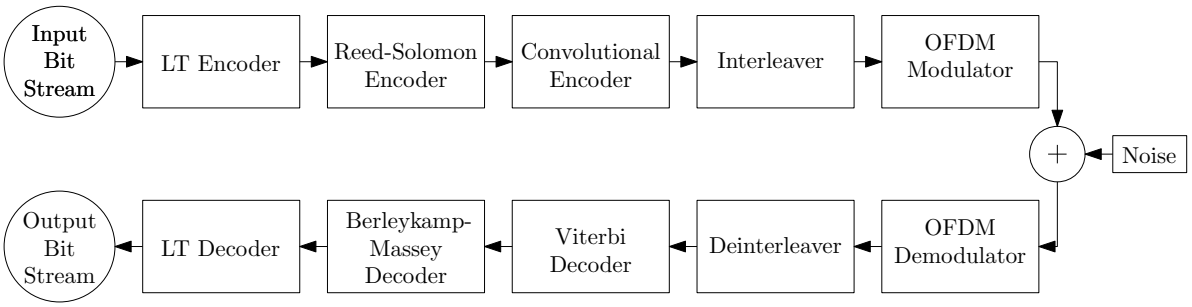


Figure 3.2: LT-modified G3 PLC system.

3.2 Forward Error Correction

This section explains the encoders and decoders which are used in all the systems of the research. Encoders which are present in the G3 benchmark system follow the specifications provided in the standard [8]. Decoders on the other hand are not specified by the standard and must therefore be chosen for this research. The criteria for the selection of decoders is based on simplicity of implementation for the codes which are

common to both sections i.e. RS code, CC and RC as this research is not focused on different implementations of these decoders.

3.2.1 LT Code

LT Code Encoder: LT codes can produce any value n of encoded packets from a value k of initial source packets [12]. At each iteration, a new encoded packet is produced by the XOR operation of d source packets picked at random from a uniform distribution. A random encoded packet degree d must thus be generated at each iteration. This value is generally produced from a probabilistic distribution. The first distribution designed with this process in mind is the ideal Soliton distribution which is defined by the PDF [12]

$$p(1) = \frac{1}{k} \tag{16}$$

$$p(d) = \frac{1}{d(d-1)} \text{ for } d = 2, 3...k \tag{17}$$

This distribution is typified by a spike at a low degree value signifying that most encoded packets are composed of a low number of packets. An example of this distribution with a k value of 50 and a spike at a value of 2 can be seen in Figure 3.3.

Due to the instability of this distribution in practice during the decoding process, it can be modified such that a second spike appearing at a larger value Q occurs, resulting in encoded packets containing more if not all of the original packets. This therefore decreases the chance of one of the initial packets not being included in any of the encoded packets. This new distribution $\mu(d)$, named the robust Soliton distribution, is obtained by performing the following modification on the ideal Soliton distribution PDF [51]

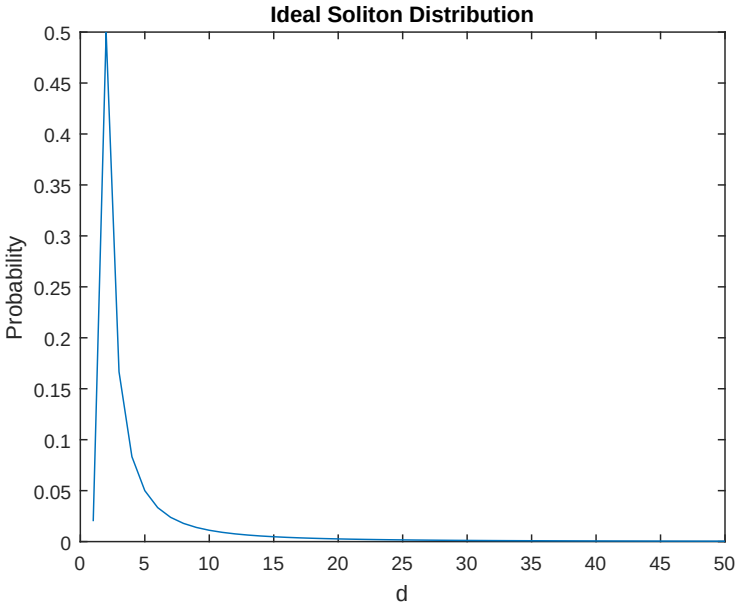


Figure 3.3: Ideal Soliton Distribution with $k = 50$.

$$\tau(d) = \frac{1}{iQ} \qquad \text{for } i = 1, 2, ..., Q-1 \tag{18}$$

$$\tau(d) = \frac{\ln(\frac{R}{\delta})}{Q} \qquad \text{for } i = Q \tag{19}$$

$$\tau(d) = 0 \qquad \text{for } i = Q+1, ..., k \tag{20}$$

$$Z = \sum_{d=1}^{k} p(d) + \tau(d) \tag{21}$$

$$\mu(d) = \frac{p(d) + \tau(d)}{Z} \tag{22}$$

It should be noted that Z is a normalisation factor ensuring the sum of the PDF is equal to one as per the PDF definition, δ is the probability of decoding failure and R is equal to $\frac{k}{Q}$. An example of this distribution with a k value of 50, Q value of 10 and a δ value of 0.05 is shown in Figure 3.4.

Another variable which needs to be specified for the LT code is the length, l, of the LT packets. The variable l is selected such that it is as small as possible and thus divide

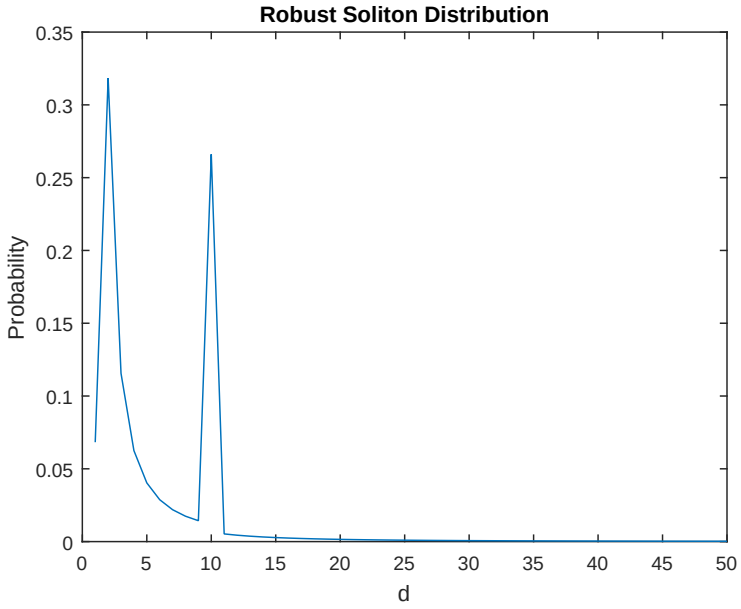


Figure 3.4: Robust Soliton Distribution with $k = 50$, $Q = 10$ and $\delta = 0.05$.

a given amount of input data into as many source packets as possible. On the other hand, it must be large enough such that the possible packet space, which is of size 2^l, is greater than the number of source packets. This condition must be met in order to avoid linearly dependent packets which provide no new information during the decoding process, i.e. resulting in matrix rows being equal to 0.

LT Code Decoder: LT codes can be decoded by an iterative message passing algorithm such as belief propagation (BP) or with techniques involving Gaussian Elimination (GE) [52]. The choice of using BP or GE for the LT decoding procedure involves a trade-off between performance and complexity [53]. Decoding using both BP and GE are implemented in this research so that they may be compared. In both cases, for the decoding operation to begin, information about which source packets have been combined in each received encoded packet is required. This information can be transmitted alongside the information data but a risk is that it can then get corrupted. Transmitting this packet combination data also slows down the data rate. For this reason, it is assumed that both transmitter and receiver have access to this prior information available to them, either generated by a pseudorandom number generator with a common seed or in the form of matching lookup tables in memory.

For BP decoding, at each iteration a new LT packet y_j, where $j \in \{1, 2, ..., n\}$, is received. The first step is to identify if the packet is of degree 1 at which point it is then considered to be a decoded packet corresponding to a source packet x_i, where $i \in \{1, 2, ..., k\}$. Packets x_i which have been decoded are then XOR'ed with any newly received or stored packets y_j that may contain it. Following this step, if the degree of any packet y_j becomes 1, the process is repeated. If the degree of a newly received packet results in a value being greater than 1, the packet is stored in a buffer for later processing. Finally if at any stage of the decoding procedure the degree of a received packet y_j becomes 0, it is deemed to be a linearly dependent packet that provides no new information to the receiver and is discarded. Decoding halts when all packets x_i are recovered or when there are no more packets y_j of degree 1. This process is illustrated in Figure 3.5.

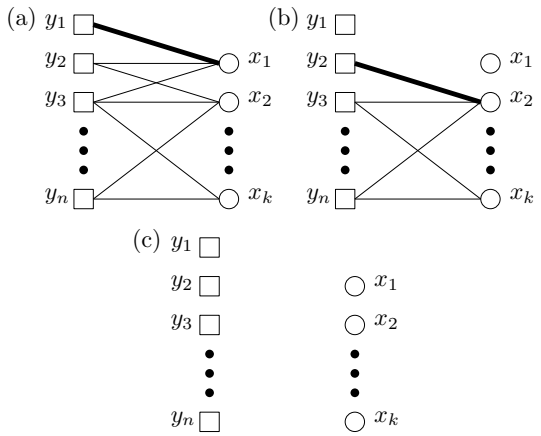


Figure 3.5: BP decoding procedure illustrated as a series of bipartite graphs. (a) y_1 identified as packet of degree 1. (b) x_1 recovered and removed from all packets y_j which contain it, y_2 identified as new packet of degree 1. (c) Decoding process terminated, all source packets recovered.

Contrary to decoding using BP, the GE method does not have the constraint of requiring packets of degree 1 at each iteration of the decoding procedure. Instead, decoding can be accomplished once k linearly independent encoded packets are received. A set of equations is first set up in the form $Ax = b$. The elements of matrix A are 1 if packet x_i, where $i \in \{1, 2, ..., k\}$, is part of encoded packet y_j, where $j \in \{1, 2, ..., n\}$, and are 0 if it is not. The vector x represents all the source packets x_i and the vector b represents the encoded packets y_j. An example of the GE procedure using the same

source and encoded packet set-up as in Figure 3.5 is shown in Figure 3.6.

$$(a)\begin{bmatrix}1 & 0 & \dots & 0\\ 1 & 1 & \dots & 0\\ 1 & 1 & \dots & 1\\ \vdots & \vdots & \ddots & \vdots\\ 0 & 1 & \dots & 1\end{bmatrix}\begin{bmatrix}x_1\\ x_2\\ \vdots\\ x_k\end{bmatrix}=\begin{bmatrix}y_1\\ y_2\\ y_3\\ \vdots\\ y_n\end{bmatrix}$$

$$(b)\begin{bmatrix}1 & 0 & \dots & 0\\ 0 & 1 & \dots & 0\\ 0 & 0 & \dots & 1\\ \vdots & \vdots & \ddots & \vdots\\ 0 & 0 & \dots & 0\end{bmatrix}\begin{bmatrix}x_1\\ x_2\\ \vdots\\ x_k\end{bmatrix}=\begin{bmatrix}y'_1\\ y'_2\\ y'_3\\ \vdots\\ y'_n\end{bmatrix}$$

$$(c)\begin{bmatrix}1 & 0 & \dots & 0\\ 0 & 1 & \dots & 0\\ 0 & 0 & \dots & 1\\ \vdots & \vdots & \ddots & \vdots\\ 0 & 0 & \dots & 0\end{bmatrix}\begin{bmatrix}x_1\\ x_2\\ \vdots\\ x_k\end{bmatrix}=\begin{bmatrix}x_1\\ x_2\\ x_3\\ \vdots\\ 0\end{bmatrix}$$

Figure 3.6: GE decoding procedure overview. (a) Received packets inserted into matrix. (b) A matrix is triangulated and (c) back-substitution is performed to obtain original source packets.

3.2.2 Reed-Solomon Code

RS Encoder: RS codes are a type of block code which generate codewords composed of n_{RS} symbols from an input message containing k_{RS} symbols [43]. The number of bits contained in a single symbol depends on the Galois Field order i.e. an RS symbol composed of m bits is constructed over $GF(2^m)$. The field generator polynomial is a primitive polynomial used to generate all of the α values and is given by [8]

$$p(x) = 1 + X^2 + X^3 + X^4 + X^8 \tag{23}$$

The G3 system can use two different RS code versions, namely a (255, 239, 8) code or a (255, 247, 4) code which are both implemented in systematic form. Systematic form means that the message used to obtain a codeword is contained within it without modifications, i.e. parity bits are simply appended at pre-decided locations to form the

codeword. In the code description brackets, the third value is the parameter t which is the error correcting capability of the code and which is obtained by calculating $t = \frac{n-k}{2}$. The generator polynomial used to generate the codewords is then [8]

$$\boldsymbol{g}(X) = \prod_{i=1}^{2t}(x - \alpha^i). \tag{24}$$

The $n_{RS} - k_{RS}$ parity bits to be appended to the message for a codeword in systematic form are then obtained by computing the remainder as follows:

$$\boldsymbol{s}(X) = \boldsymbol{m}(X) \cdot X^{(n_{RS}-k_{RS})} \bmod \boldsymbol{g}(X) \tag{25}$$

where $\boldsymbol{m}(X)$ is the message polynomial to be encoded. The multiplication by $X^{(n_{RS}-k_{RS})}$ serves as a shift to change the message position. The encoded message can then be obtained by adding the remainder and shifted message

$$\boldsymbol{c}(X) = \boldsymbol{s}(X) + \boldsymbol{m}(X) \cdot X^{(n_{RS}-k_{RS})} \tag{26}$$

RS Decoder: There are various methods which can be used to decode RS codes which can either be of a soft or hard decoding nature. A hard decision decoder using the Berleykamp-Massey algorithm is used in the implementation as this component is common to all systems being tested and is not the focus of the research for an improvement in performance. Furthermore, this results in a simpler coding implementation. In this algorithm, both the error locations as well as their values must be identified which allows for the correcting of errors provided only t or less symbols have been affected. This code is good for both random errors and burst errors as each symbol covers a sequence of m bits.

RS Code Shortening: A technique known as code shortening is used to increase the data rate of the system depending on the throughput required. An example of RS shortening taken from one of the benchmark system case used for this research is the following: k_{short} bytes of data (235 bytes) to be transmitted is appended with a sequence of zeros until a new sequence of length k_{RS} (239 bytes) is obtained. This new sequence is then encoded using the RS (255, 239, 8) encoder which generates a systematic codeword. The zeros that have been appended are then removed followed by the transmission of

the original data and new parity bits. Once arrived at the receiver, zero padding is once again added such that decoding can be performed by the RS (255, 239, 8) decoder. Once the decoding operation has been completed, the zeros are removed to obtain the final decoded data. This sequence of events is illustrated in Figure 3.7.

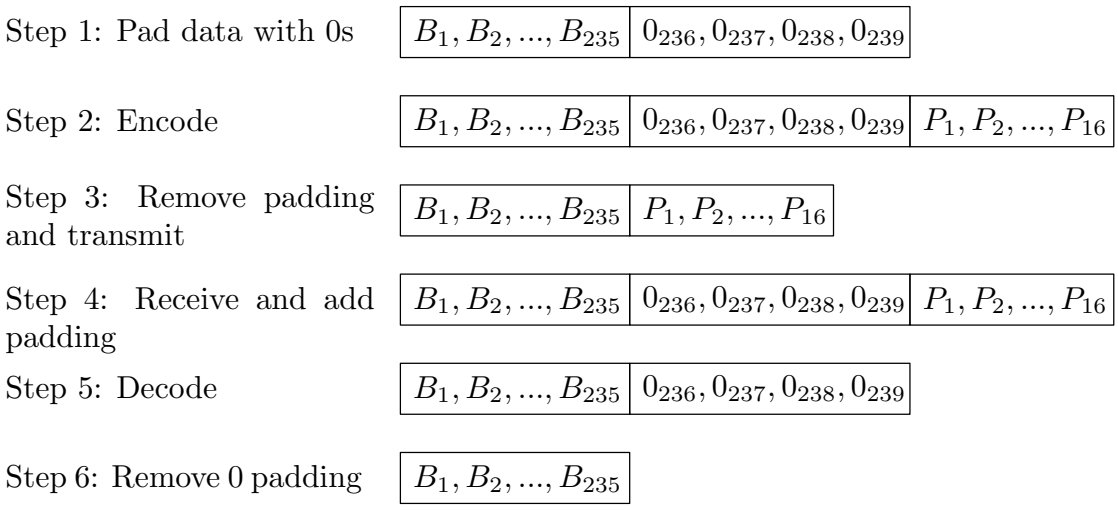


Figure 3.7: RS code shortening procedure.

The drawback of this method is that the overall performance of the system decreases as the code shortening is increased [54]. This performance trade-off is due to the fact that the error correcting capabilities of the code remains the same, i.e. $t = 8$ for both the shortened and non-shortened code, but that the shortened code then operates on a smaller number of binary information data, i.e. a higher E_b/N_0 value is required for a shortened code to have equal performance as a non-shortened code when the E_s/N_0 is normalised by the code rate.

3.2.3 Convolutional Code

CC Encoder: As opposed to block codes such as RS which operate on chunks of binary data of a specific size, CC operate on a bit stream which can be of any size [55]. Similarly to other types of codes, CC possess a code rate where n_{CC} bits are generated from an input of k_{CC} bits. On the other hand, their performance can be improved through the increase of a variable L (memory order + 1) representing the constraint length of the system which has no effect on the rate of the code but increases complexity. In the G3 system, the convolutional code used is a half-rate code which has a constraint

length L value of 7 (memory order of 6) and is defined by the generator polynomials

$$\boldsymbol{g}^{(0)} = (1\ 1\ 1\ 1\ 0\ 0\ 1) \tag{27}$$

$$\boldsymbol{g}^{(1)} = (1\ 0\ 1\ 1\ 0\ 1\ 1) \tag{28}$$

In the generator polynomials, binary digits with the value of 1 signify an active connection from the stored data to the XOR operation and a value of 0 signifies the lack of a connection. A generator polynomial is defined for every output bit of the encoder. The block diagram of the G3 CC encoder can be seen in Figure 3.8.

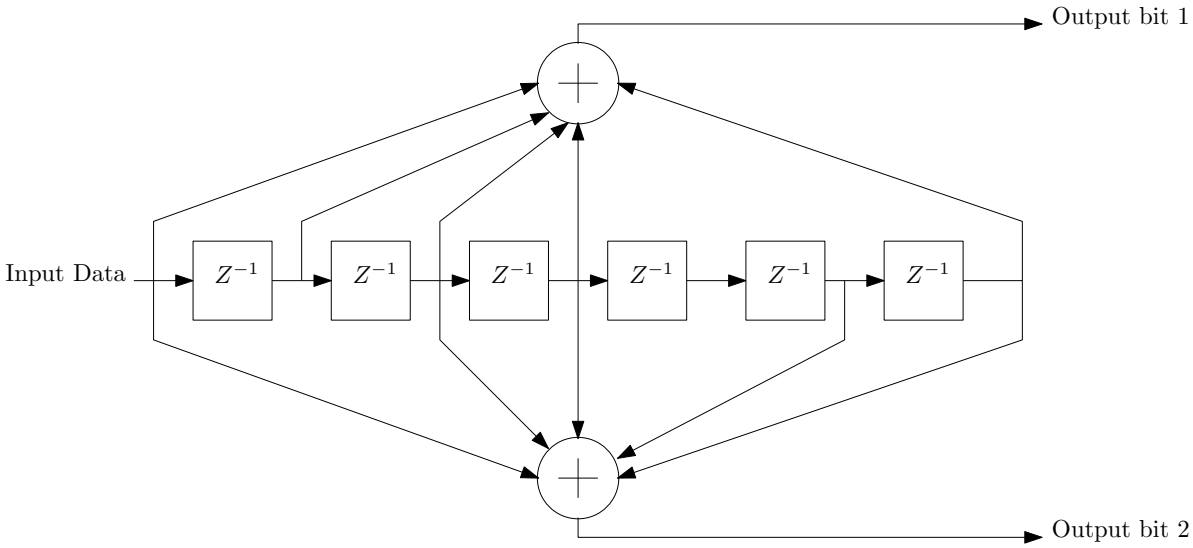


Figure 3.8: Half-Rate convolutional encoder with L value of 7 and generator $\mathbf{g} = [171\ 133]$ in octal form.

The free distance d_{free} of this code is 10 resulting in an error correcting capability t of 4 within a reasonable frame size since $t = \lfloor \frac{d_{free}-1}{2} \rfloor$. This code is thus not good at correcting errors that are closely grouped together such as in the event of a burst error but rather is potent at correcting random errors which are spread out. In this implementation zero-termination is used which means that at the end of the binary sequence to be encoded is padded a sequence of $L - 1$ all zero bits. This trailing sequence is added such that the encoder can be reset to the all zero state every time the encoding procedure is terminated. This allows the initial state of the encoder to be known by the receiver at the beginning of each frame. Because zero termination is used,

special care needs to be taken when normalising to obtain the BER vs E_b/N_0 curve. The new effective rate is calculated as follows [56]

$$R_{effective} = R\left(1 - \frac{L-1}{r+L-1}\right) \tag{29}$$

where r is the size of the un-padded bit stream frame input to the convolutional encoder and L is as previously defined. From (29) it can be seen that the fractional rate loss decreases the larger the value of r is. This therefore makes the fractional rate loss negligible when a large number of bits is used such as in G3 systems where r varies between 168 and 1128 which results in $R_{effective} \approx \frac{1}{2}$ in this case.

CC Decoder: Decoding of convolutional codes can be achieved by various techniques but is typically performed using the Viterbi algorithm [43]. Viterbi algorithm decoding is a maximum likelihood decoding algorithm which can be implemented either with hard or soft decision decoding. The reason for this decoder algorithm choice is that it is simple to implement and binary sequences can be decoded quickly provided that L is not too high. As stated previously, the criteria for the decoder implementation selection is simplicity since this code is used in both the benchmark G3 system and LT-modified G3 system resulting in hard decision decoding being used. To accelerate the speed performance of the Viterbi algorithm, it can be made to act on a truncated part of the whole binary sequence which is to be decoded [43]. It has been shown that a significant increase in speed can be achieved with minimal loss in performance when a truncation window also known as the traceback length equal to 5 times the constraint length L is used [57].

3.2.4 Repetition Code

RC Encoder: RCs operate by repeating binary data that enters the encoder a specified amount of n_{rep} times. The rate of RCs is thus $\frac{1}{n_{rep}}$. In the case of G3 systems, the amount of repetition is 4 for the information data and 6 for the frame control header (FCH). As control messages are not required for the purpose of this research, a (4, 1) RC is used as it is assumed that only information data is being transmitted. For example, let the binary vector

$$\mathbf{u} = \{u_0, u_1, u_2, u_3\} \tag{30}$$

of length 4 bits be input to the (4, 1) RC encoder. The output vector which is produced by the encoder is then

$$\mathbf{v} = \{u_0^1, u_0^2, u_0^3, u_0^4, u_1^1, u_1^2, u_1^3, u_1^4, u_2^1, u_2^2, u_2^3, u_2^4, u_3^1, u_3^2, u_3^3, u_3^4\} \tag{31}$$

where the superscript represents the repetition index.

RC Decoder: RCs can be decoded by a soft or hard decision majority logic decoder [58]. Majority logic decoders operate by looking at the sequence of bits in a codeword and selecting the binary digit that occurs the most. In the case of a tie, it can be assumed that either an erasure has occurred or a bit can be selected at random. As the G3 system functions with an n_{rep} value of 4, the decoding logic for this case is shown in Table 2.

3.2.5 Interleaver

Encoder: The G3 interleaver interleaves data both in time across OFDM symbols and in frequency across OFDM subcarriers [8] as opposed to the typical block interleaver described in Section 2.3.1 which interleaves the data in time only. Given a matrix of dimension $N_{sc} \cdot N_{sym}$, the new interleaved coordinates (I, J) of a bit with original coordinate (i, j), where $i \in \{0, 1, ..., N_{sc} - 1\}$, and where $j \in \{0, 1, ..., N_{sym} - 1\}$, is given by

$$J = (j \cdot n_j + i \cdot n_i) \bmod N_{sym} \tag{32}$$

$$I = (i \cdot m_i + J \cdot m_j) \bmod N_{sc} \tag{33}$$

where for successful operation n_i, n_j, m_i and m_j are selected such that the following conditions hold:

Table 2: (4, 1) repetition code majority logic decoding rule.

Received binary sequence	Decoded binary sequence
0000	0
0001	0
0010	0
0011	random/erasure
0100	0
0101	random/erasure
0110	random/erasure
0111	1
1000	0
1001	random/erasure
1010	random/erasure
1011	1
1100	random/erasure
1101	1
1110	1
1111	1

$$n_i, n_j < N_{sym} \tag{34}$$

$$m_i, m_j < N_{sc} \tag{35}$$

$$\text{GCD } (m_i, N_{sc}) = \text{GCD } (m_j, N_{sc}) = \text{GCD } (n_i, N_{sym}) = \text{GCD } (n_j, N_{sym}) = 1 \tag{36}$$

An example with an N_{sym} value of 4, N_{sc} value of 4, n_i value of 1, n_j value of 3, m_i value of 3 and m_j value of 1 is given in Figure 3.9.

Decoder: The de-interleaver functions by reversing the process of the interleaver. Namely, it reverses the process by going from Figure 3.9 b) to Figure 3.9 a).

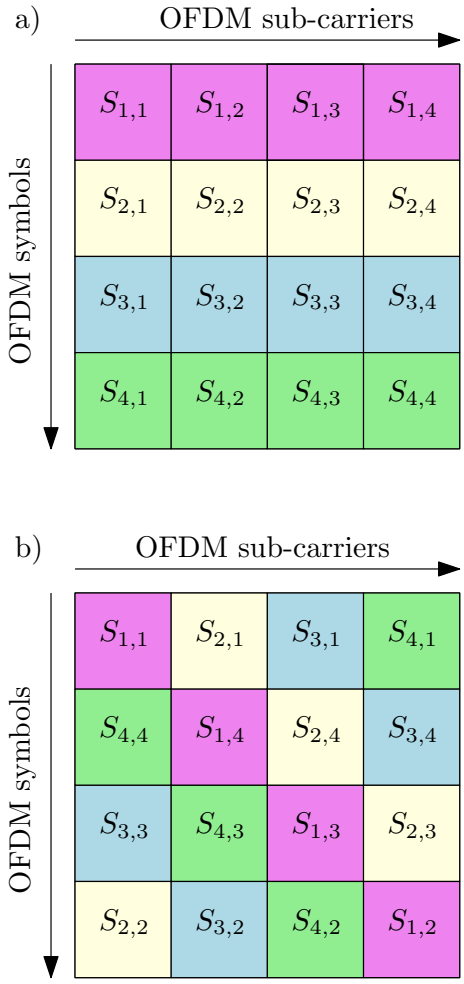


Figure 3.9: G3 block interleaving example. a) Original binary data. b) Interleaved binary data.

3.3 Channel Model

The PLC channel block takes as input the signal transmitted from the transmitter and outputs a noisy version of the signal which is then sent to the receiver. In order to simulate a noisy PLC channel, two of the noises described in Section 2.2, namely BN and IN are implemented in the block. NBI is not implemented as it is assumed that it can be avoided. This assumption is made from the fact that NBI occurs at specific frequencies such as TV scanning frequencies which means that they affect a subset of the total OFDM sub-carriers. NBI can be avoided by the adaptive tone mapping feature of G3 systems which specifies the sub-carriers to be used following channel estimation. Furthermore, signal attenuation which is dependent on cable length between transmitter and receiver is also ignored as it is assumed that perfect repeaters and channel estimation

are used to counteract this problem in order to simplify the simulation.

3.3.1 Background Noise

Background noise is generated from the method described in Section 2.2.1. As the performance measurement is based on the E_b/N_0 values, careful attention must be given for this type of noise to ensure correctness of the results. The plots of BER vs E_b/N_0 for simple systems such as ones using no FEC and systems only using RS only were obtained from simulations and compared to theoretical BER curves obtained from standard communications textbooks and found to match. Once the noise signal $n(t)$ is generated over the same time period as the clean signal $s(t)$, the result is a signal of the form

$$s_{noisy}(t) = s(t) + n(t) \tag{37}$$

Once this step is completed, the composite signal is ready to be sent to the impulse noise generating module.

3.3.2 Impulse Noise

The impulses are generated from (9) where each variable in the equation is randomly generated during each simulation run. The impulse arrival times, $t_{arr,i}$, are calculated based on the inter-arrival times generated from a Poisson process in which the λ parameter takes values between 67 and 334 [16]. This results in an average inter-arrival time between impulses ranging between 0.015 s and 0.003 s for a worst case scenario. The set of impulse amplitudes A_i are generated by the similar process used to generate the BN but instead can take an amplitude 50 dB greater than that of the BN thus overpowering the signal. Finally, the impulse width $t_{w,i}$ is uniformly distributed with a duration between 10 μs and 1 ms. Once the impulses have been generated for the same amount of time as the noisy transmitted signal, they are added together resulting in the following signal sent to the receiver.

$$r(t) = s(t) + n(t) + s_{IN}(t) \tag{38}$$

3.4 Digital Modulation

Information data can be transferred across a medium by modulating a waveform that can traverse it such as electromagnetic waveforms in the case of radio communications or a voltage waveform in the case of PLC. Thus to transmit data through the PLC channel, a modulation scheme is required which converts the binary data to be transferred into a voltage signal $s(t)$ in time suitable for travelling across copper conductors. In the case of G3 systems, this is achieved through the use of an OFDM transmitter and receiver in conjunction with BPSK, DBPSK or DQPSK depending on the chosen settings.

3.4.1 Single Carrier Modulation

Single carrier modulation involves varying characteristics of a carrier waveform such as its amplitude A, its phase θ, its frequency f or a combination of those [59]. In the case of G3 systems, this is achieved by varying θ which results in phase-shift keying (PSK). Phase modulation can either be of a differential or non-differential nature and has a varying modulation order value M. The baseband representation of M-PSK signals is

$$D_i = e^{j\theta + \frac{j2\pi m_i}{M}} \qquad m_i = 0, 1, ..., M-1 \tag{39}$$

For the BPSK modulation used in the G3 system, the M value is therefore 2 with two possible phase outputs seperated by 180°. This can be represented visually in the form of a constellation diagram as shown in Figure 3.10.



Figure 3.10: BPSK constellation diagram.

In the case of M-DPSK, the first symbol is represented using the same equation as for M-PSK modulation, i.e. (39), but the subsequent symbols each depend on the phase of the previous symbols and are thus mathematically represented in baseband form as

$$D_i = (e^{j\theta + \frac{j2\pi m_i}{M}})(e^{j\theta + \frac{j2\pi m_{i-1}}{M}}) \qquad m_i = 0, 1, ..., M-1 \tag{40}$$

As with the M-PSK modulation scheme, M-DPSK can be represented under the form

of a constellation diagram. The DBPSK constellation is identical to that of BPSK in Figure 3.10, but DQPSK contains an extra two points as shown in Figure 3.11.

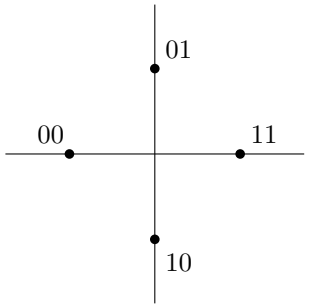


Figure 3.11: DQPSK constellation diagram.

It can be seen that Gray encoding is used where adjacent points on the constellation only have a single bit difference in order to minimise errors during decoding. In this research, DBPSK modulation is used as it is the modulation type specified for systems which are more robust and which make use of a time diversity technique. The drawback is that this results in systems with a slower data rate. The advantage on the other hand is that these systems have a better performance since the points on the constellation are separated by a larger Euclidean distance when assuming that the transmission power remains the same.

3.4.2 Orthogonal Frequency-Division Multiplexing

As opposed to single carrier modulation which obtains higher data rates by increasing the bandwidth or modulation order used for the communication, OFDM uses multiple orthogonal carriers in parallel spread across the available bandwidth [60]. OFDM can thus be regarded as the parallel concatenation of several different single carrier modulation schemes operating at different central frequencies which are orthogonal to each other. This is useful in the case where channels have a varying frequency response as each carrier then operates on a smaller bandwidth which can be considered linear. Carriers operating in the frequency region affected by deep fading can also be ignored therefore maximising the usage of the available power and bandwidth. The typical OFDM time signal representing a single OFDM symbol unaffected by noise is

$$s(t) = \frac{1}{\sqrt{N}} \sum_{i=0}^{N_{sc}-1} S_i e^{2\pi f_i t} \tag{41}$$

where N_{sc} is the number of sub-carriers in the system, f_i is the central frequency of the i^{th} sub-carrier and S_i is a set of complex values representing the single carrier baseband modulated symbols. A G3 system typically transmits frames which possess a varying number of consecutive OFDM symbols N_{sym} taking discrete values in the range of 40 to 252 symbols resulting in data rates from 2423 bit/s to 5592 bit/s. The block diagram representing the modulator and demodulator can be seen in Figure 3.12 and Figure 3.13 respectively.

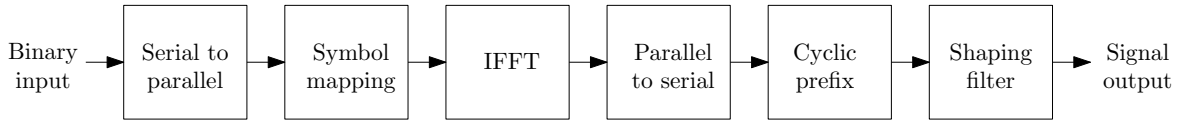


Figure 3.12: OFDM modulator block diagram.

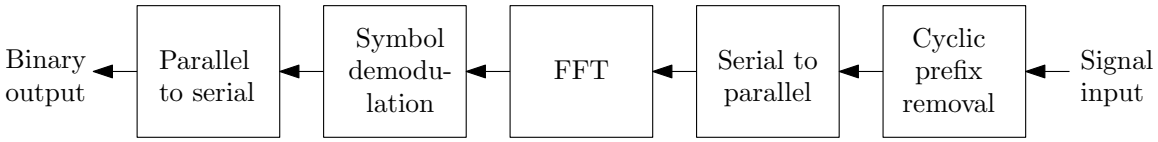


Figure 3.13: OFDM demodulator block diagram.

Modulator: The first step in the OFDM modulator is a serial to parallel converter which takes as an input a binary stream from the FEC section and which distributes it evenly according to the number of sub-carriers used. In the case of G3 systems, this amounts to a total of 36 sub-carrier channels. In the symbol mapping section, each parallel stream is then modulated according to the single carrier modulation scheme of choice which is DBPSK in this case. The DBPSK system configuration is chosen as it is the one which results in the most robust system options possible. The baseband modulated signals are then fed to the 256 inputs of the IFFT where each input of the IFFT represents one of the sub-carriers. IFFT inputs associated with sub-carriers which are not in use are simply fed with an all 0 input and ignored during the demodulation process. Following the IFFT, the time points generated from the IFFT are converted from a parallel stream to a serial stream according to the sampling rate f_s equal to 0.4

MHz used in the system. In the cyclic prefix step, a cyclic prefix extension of length N_{cp} is added between each OFDM symbol to prevent inter symbol interference (ISI). In this case, it is achieved by copying the last 30 time samples of the current OFDM symbol and pre-pending them to it. In the final step of the OFDM modulator, N_{win} sample points at the edge of each OFDM symbol are shaped according to a raised cosine window for reduction of the side-lobes in the frequency domain and the out of band emissions. The raised cosine window is performed in the time domain by multiplying the first and last 8 samples of each OFDM symbol by the values shown in Table 3.

Table 3: G3 raised cosine window sample multipliers.

Sample number	Front sample multiplier	Tail sample multiplier
1	0	0.9619
2	0.0381	0.8536
3	0.1464	0.6913
4	0.3087	0.5
5	0.5	0.3087
6	0.6913	0.1464
7	0.8536	0.0381
8	0.9619	0

It should be noted that in a real world communication system, the signal would then be up-converted to the required frequency range by the transmitter and down-converted back to baseband by the receiver. This up and down conversion process is not necessary for the purpose of this research thus resulting in the simulations being performed at baseband.

Demodulator: The OFDM demodulator operates by performing the inverse process performed by the OFDM modulator, i.e. transforming the received time signal back into binary data. Theoretically, the first step would consist of performing carrier recovery and symbol synchronisation due to carrier frequency offsets and symbol timing offset that might be caused by the channel characteristics. As both of these processes are

outside the scope of this research, they are ignored, i.e. it is assumed that perfect symbol synchronisation and carrier frequency information are available to the receiver at all times. In the simulation, the first step is therefore to remove the cyclic prefix by discarding the first 30 samples of each symbol. The time sample points are then converted into parallel format such that they may be fed to the inputs of the FFT block which reverses the operation performed by the IFFT. This is because

$$\text{FFT}(\text{IFFT}(S_i)) = S_i \tag{42}$$

Demodulation of every output from the FFT block can then be performed according to the modulation scheme used in the system which is DBPSK in this case. It should be noted that the FFT outputs representing the sub-carriers which are not in use are simply ignored. In the final stage, the binary data obtained from the symbol demodulation block is converted from a parallel stream to a serial stream ready to be decoded by the receiver. The overall OFDM transceiver characteristics used in this research are summarised in Table 4.

Table 4: OFDM transceiver specifications summary.

Specification	Value	Symbol
FFT size	256	N_{fft}
Cyclic prefix length	30 samples	N_{cp}
Sampling rate	0.4 MHz	f_s
Sub-carriers	36	N_{sc}
Windowing	Raised cosine	-
Window length	8 samples	N_{win}
Symbols per frame	40 - 252	N_{sym}
Modulation Scheme	DBPSK	-

Chapter 4: Comparative Study of a Time Diversity Scheme Applied to G3 Systems for Narrowband Power-Line Communications

The results of the journal article which has been submitted to the *IEEE Transactions on Consumer Electronics* are presented in this chapter. Herewith, the performance and complexity of narrowband PLC systems provided by the G3 PLC standard are analysed when concatenated with an LT code. It is shown that an improvement in BER is obtainable under non worst-case channel conditions with an increase in system complexity. It is then demonstrated that this increase in complexity is higher on the receiver side whilst being negligible on the transmitter side signifying that it can be well tolerated in systems which utilise it such as AMR systems. This is due to the star topology of the network meaning that the receiver which comes with more built-in resources can accommodate the increase in complexity. The reference to the paper is currently the following until acceptance by the peer-review process:

> **Y.F. Rivard** and L. Cheng, "Comparative Study of a Time Diversity Scheme Applied to G3 Systems for Narrowband Power-Line Communications", currently submitted to the *IEEE Transactions on Consumer Electronics* for the peer-review process as of 23/05/2016.

The main research idea was derived from a joint effort of **Y.F. Rivard** and Prof. Ling Cheng, inspired by his previous works on PLC. The software implementation used for the collection of data was fully coded by **Y.F. Rivard**. The journal article was written by **Y.F. Rivard** whilst Prof. Ling Cheng supervised the research and ensured the journal article met the required high quality standards for international publication.

4.1 Current Industry Standard G3 Simulation Performance Analysis

To establish a baseline, simulations are first run with G3 systems provided by the standards. Three different G3 systems are tested to cover the range of system specifications containing time diversity under the form of RC. These systems are therefore based on implementations with an N_{sym} value of 40, 56 and 252 OFDM symbols resulting in data rates of 2423 bit/s, 3257 bit/s and 5592 bit/s respectively. The G3 systems are then tested over three PLC channels which have different impulse rate characteristics i.e. worst case scenario ($\lambda = 1/0.003$), best case scenario ($\lambda = 1/0.015$) and the midpoint ($\lambda = 1/0.009$). The benchmark results can be seen in Figure 4.1, Figure 4.2 and Figure 4.3.

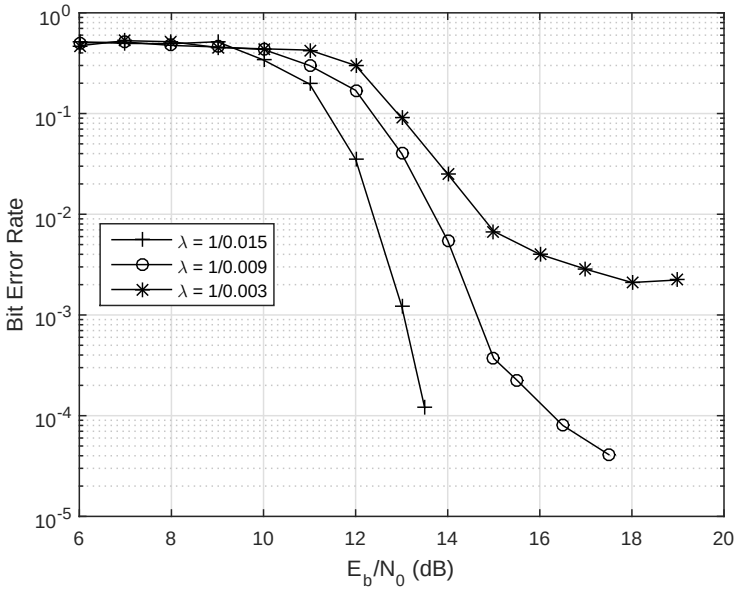


Figure 4.1: BER vs E_b/N_0 for G3 system with 40 OFDM symbols and (21, 13) RS over PLC channel with varying impulse rate parameter.

From these results, it can be concluded that the presence of IN in the PLC channel results in a performance behaviour different from channels with AWGN only. Specifically, a noise floor is present following the initial waterfall region which occurs at different E_b/N_0 and bit error rate (BER) values depending on the system code specifications. As λ increases, the occurrence of impulses increases resulting in a worse performance. As the N_{SYM} value decreases, so does the performance. This behavior is due to the fact that as N_{SYM} is lowered, the code rate of the RS code gets lowered whilst the error

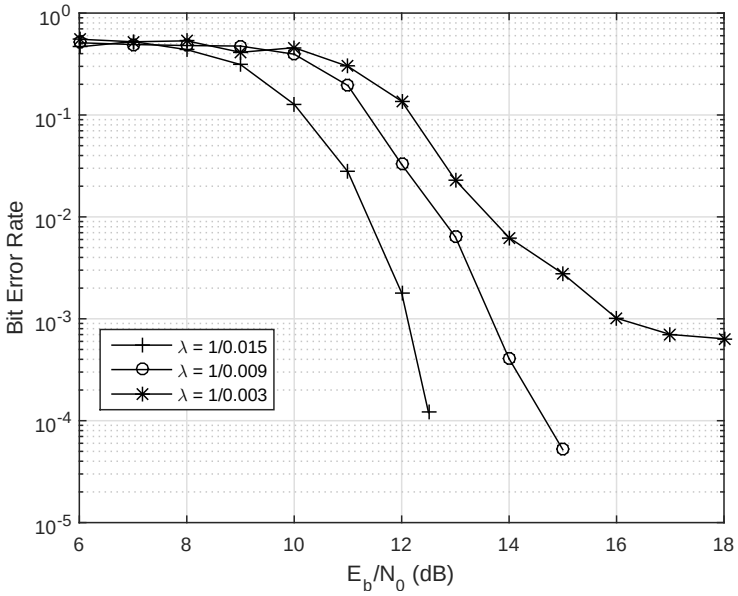


Figure 4.2: BER vs E_b/N_0 for G3 system with 56 OFDM symbols and (30, 22) RS over PLC channel with varying impulse rate parameter.

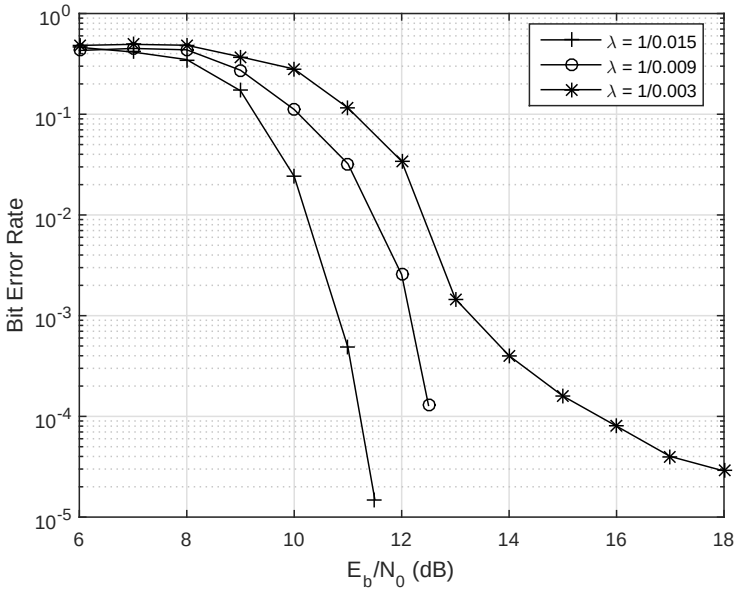


Figure 4.3: BER vs E_b/N_0 for G3 system with 252 OFDM symbols and (141, 133) RS over PLC channel with varying impulse rate parameter.

correcting capability stays the same therefore resulting in a smaller energy per bit value E_b and thus worsening the performance [54].

4.2 LT-Modified G3 System Performance Analysis

Simulations are performed to determine the behaviour of this new scheme on the PLC channel under the same conditions as those used previously i.e. N_{sym} values of 40, 56 and 252 with λ values of 1/0.015, 1/0.009 and 1/0.003 whilst keeping the RS code rates associated with systems of different OFDM symbol lengths constant. To implement these systems, the number of LT source packets k and the robust Soliton distribution variables must first be selected. Generally, it is proven that LT codes perform better as the amount of source packets k is increased [16]. In the case of G3 systems, this could be achieved by splitting data from the LT transmitter across multiple frames but the drawback would be added non-negligible latency. To prevent this and adhere to the G3 specifications as much as possible, LT encoded data is restricted to a single frame. It should be kept in mind that due to this constraint the number of total available bits per frame is dictated by the frame size which is of $N_{sc} \cdot N_{sym} \cdot M$ bits. For the robust Soliton distribution, a δ value of 0.02 is typically chosen [16] with a spike value Q dependent on the number of source packets chosen in each system. In these scenarios, the Q values resulting in the best performance occur at 10, 20 and 50 for the systems with an N_{SYM} value of 40, 56 and 252 respectively. The smallest practical l value in all system cases is of 10. Following this, the optimal LT data rates must then be selected for all systems. As performance is analyzed based on the BER vs E_b/N_0 values, there exists a relation between performance and data rates for both decoder implementations as shown in Figure 4.4 and Figure 4.5.

As observed, for the LT modified G3 system with an N_{SYM} value of 252 and using BP, the best code rate found that can be used is 1/1.4. For the LT modified G3 system using GE it is 1/1.05. The sharp increases and decreases observed are due to a trade-off between the amount of available LT packets and the ratio of E_s/N_0. The same process must be repeated for every system with a different N_{SYM} value as this varies in each case. To understand the difference in behavior of the two decoding methods, tests are performed by collecting samples of how many packets are required at every iteration for successful decoding when packets are being continuously transmitted. From this data the CDF of the decoding probability depending on the code rate is plotted. An example of the results obtained from systems with 252 OFDM symbols and 304 LT source packets

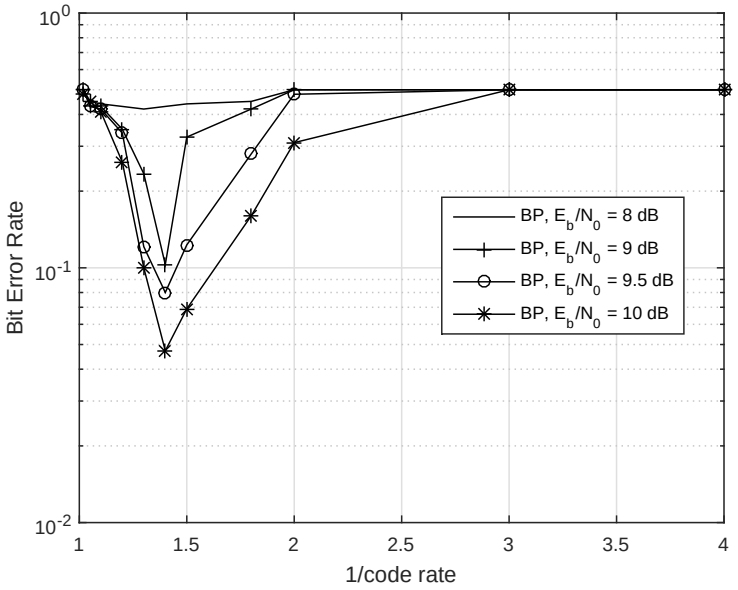


Figure 4.4: Performance depending on code rate at various E_b/N_0 values for LT-modified G3 system with 252 OFDM symbols, (141, 133) RS code, λ value of 1/0.015 and a Q value of 50 using a BP decoder.

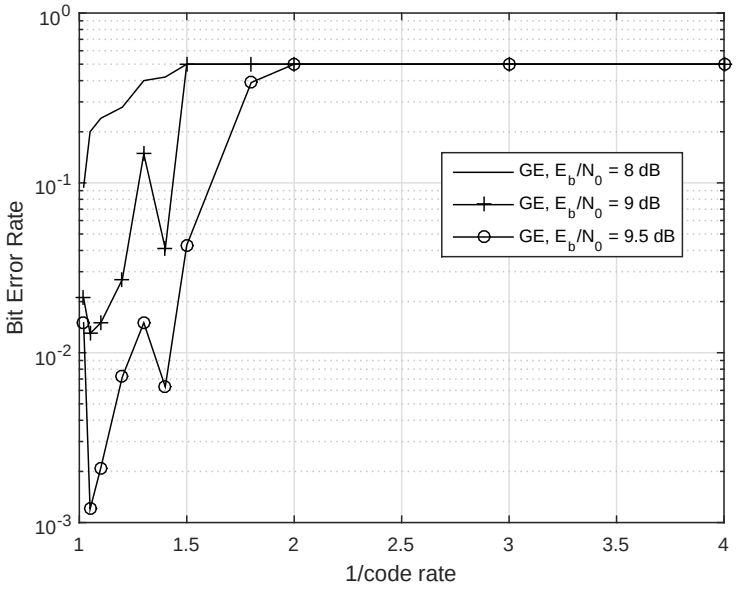


Figure 4.5: Performance depending on code rate at various E_b/N_0 values for LT-modified G3 system with 252 OFDM symbols, (141, 133) RS code, λ value of 1/0.015 and a Q value of 50 using a GE decoder.

for both decoder implementations are shown in Figure 4.6 and Figure 4.7 for comparison.

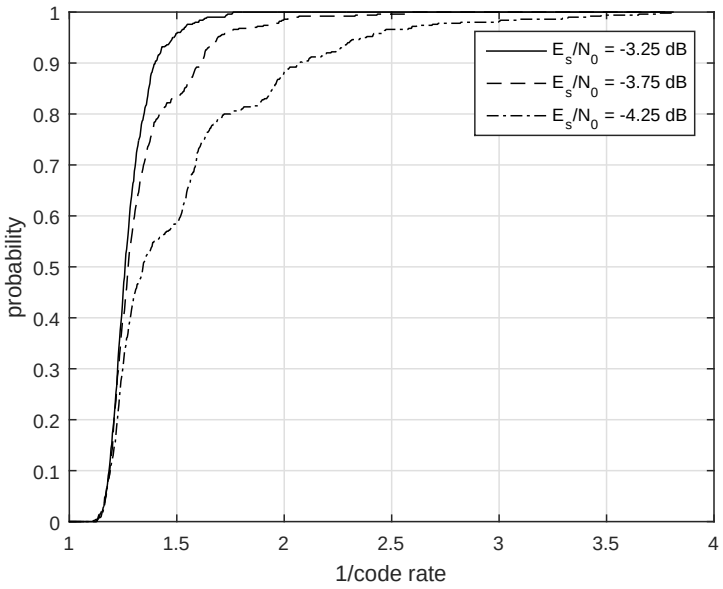


Figure 4.6: Decoding probability based on LT code rate for LT-modified G3 system with 252 OFDM symbols, (141, 133) RS code, λ value of 1/0.015 and a Q value of 50 using a BP decoder.

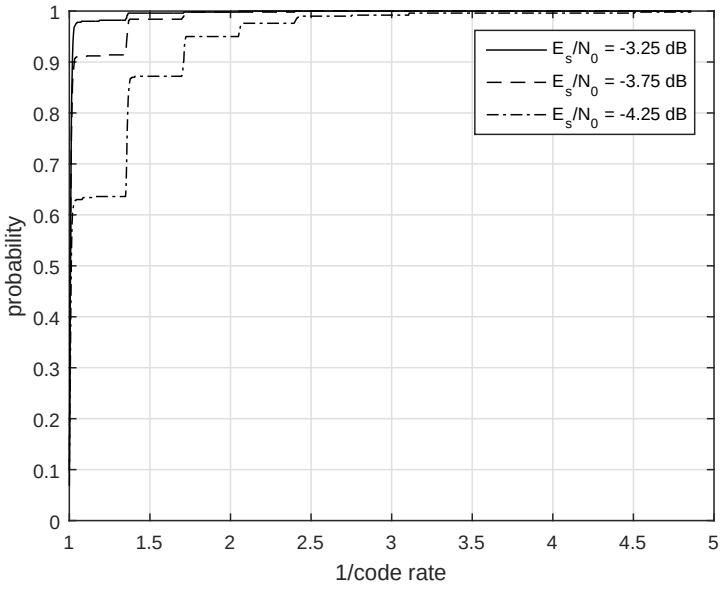


Figure 4.7: Decoding probability based on LT code rate for LT-modified G3 system with 252 OFDM symbols, (141, 133) RS code, λ value of 1/0.015 and a Q value of 50 using a GE decoder.

This series of graphs represent 3 points along the E_s/N_0 range where the waterfall occurs. E_s/N_0 values lower than those shown result in an unusable system with a BER

of 0.5 whilst higher values result in a CDF with a faster rise time. It should be reminded that in this example due to the frame size limitations and the selected source packet value k of 304, that code rate values greater than 1/1.4 cannot be used as this would result in the LT code data being sent through multiple frames, but has been shown here for the understanding that this would further increase the decoding probability for a given E_s/N_0 value. In the curves different identifiable steps can be noticed. This is explained by the fact that new LT packets arrive in bulk which are the size of a RS decoded codeword. In this new system, each frame contains 4 RS codewords since the RS code is kept constant and the removed RC has a rate of 1/4. As seen, the GE method has a probability of decoding from a much lower packet number (even when the code rate is 1) when compared to the BP algorithm decoder. This is thus the reason why the GE decoder is expected to outperform the BP algorithm decoder and why the best found data rate is at a higher value. The more gradual rise of the BP algorithm can be explained from the fact that packets are decoded progressively as encoded packets get received whilst for the GE algorithm it all gets decoded at once by solving the system of linear equations. Following this procedure for both decoder implementations the LT-modified simulation results can be observed in Figure 4.8, Figure 4.9 and Figure 4.10. The results are summarised in Table 5 where in each row representing a different test condition the best system is highlighted.

When compared to the results of the G3 systems from Figure 4.1, Figure 4.2 and Figure 4.3, a few things can be said. Firstly, it is observed that for 2 of the 18 cases, a non-negligible coding gain is observed. Both of the cases with positive results occur under the best case channel conditions with a λ value of 1/0.015 and GE decoding. The first is for the OFDM system with 252 symbols where a coding gain of up to about 1 dB can be observed followed by the OFDM system with 56 symbols where a coding gain of up to about 0.5 dB is obtained. For the rest of the systems noise floors can be examined which occur earlier than those of the unmodified G3 systems. It should also be noted that for lower values of λ, systems start performing worse as the number of OFDM symbols N_{SYM} is decreased. This behavior is once again due to the worsening performance of shortened RS codes as is the case with the benchmark systems. For cases with a higher value of λ, the situation changes and systems with a higher N_{SYM}

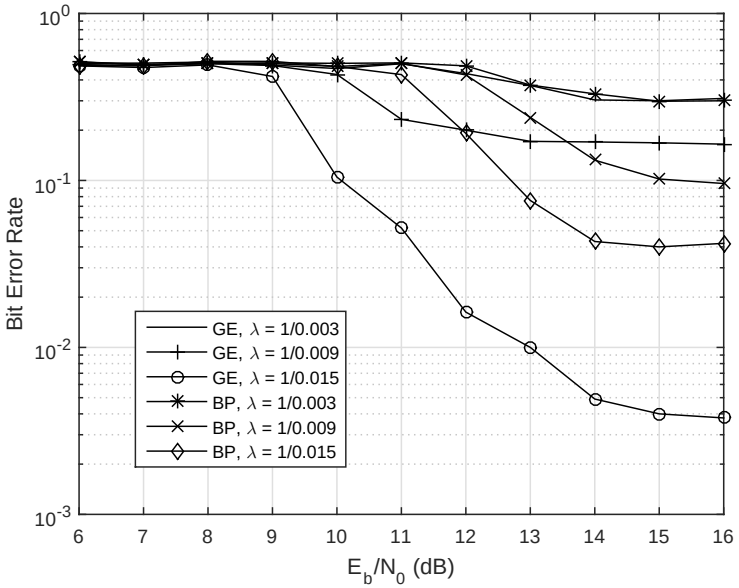


Figure 4.8: BER vs E_b/N_0 for LT-modified systems with 40 OFDM symbols, (21, 13) RS and Q value of 10 over PLC channel with varying impulse rate parameter.

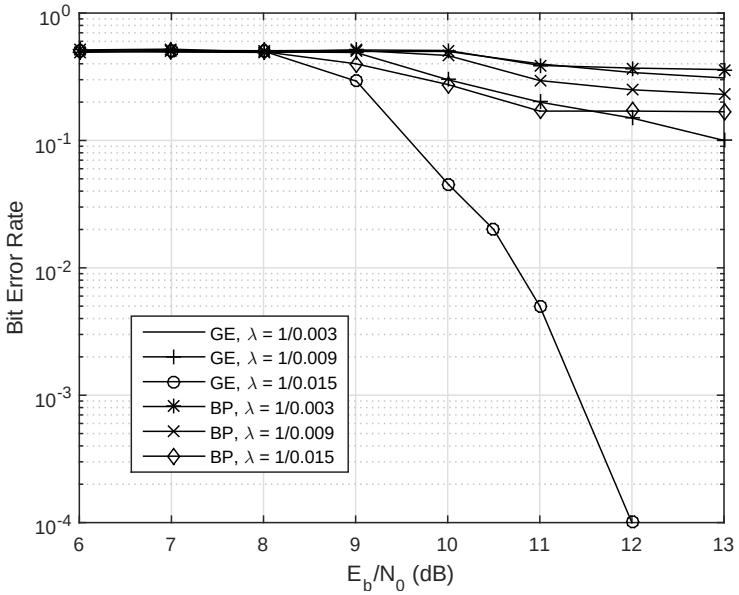


Figure 4.9: BER vs E_b/N_0 for LT-modified systems with 56 OFDM symbols, (30, 22) RS and Q value of 20 over PLC channel with varying impulse rate parameter.

value can start performing worse. The reason behind this behavior is that as the N_{SYM} value increases and thus RS codeword length increases, so does the probability of there being multiple impulses per codeword which results in a threshold of packets being corrupted beyond the decoding capability of the decoder. Finally, in some cases it can be

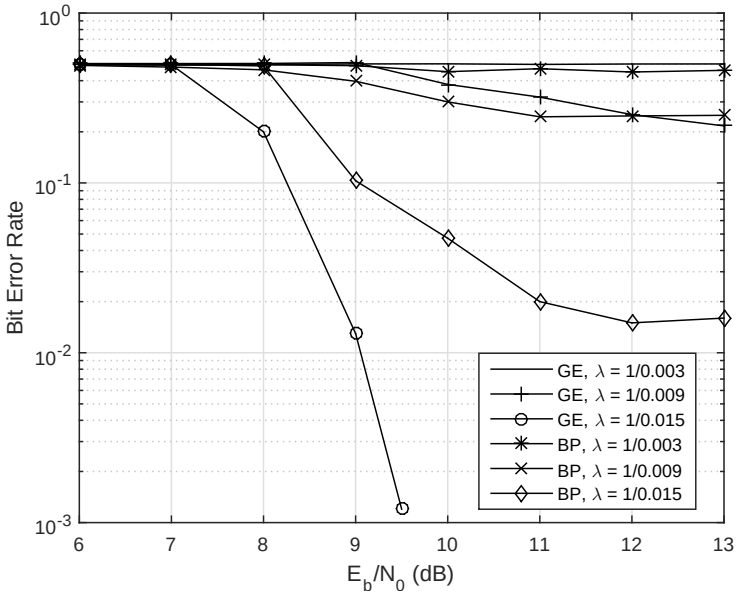


Figure 4.10: BER vs E_b/N_0 for LT-modified systems with 252 OFDM symbols, (141, 133) RS and Q value of 50 over PLC channel with varying impulse rate parameter.

seen that some systems using BP algorithm decoders slightly outperform systems using GE decoders for a given value of λ. This is due to the fact that for the BP algorithm, some packets which reach degree 1 get decoded even in the event of an overall decoding failure. On the other hand for the GE decoder, a decoding failure mostly results in a BER of 0.5. Thus for regions where decoding failures occur but some clean packets are available, the BP algorithm decoder is favorable.

The core of the problem resulting in a worse performance in most of the test cases is twofold: Firstly, the inner code is not strong enough to correct the errors and allow for the LT code to operate successfully. Secondly, not enough information is provided by the inner code for the LT decoder to pinpoint which packets have been corrupted in a batch of packets the size of a RS codeword, resulting in too many packets being discarded. Nevertheless, should it be deemed to be a worthwhile upgrade, it is recommended that an adaptive system be implemented. In this adaptive system, an LT code should be used when the channel conditions are deemed to be better than a certain threshold and the original RC should be used when the channel conditions are below that same threshold, resulting in a system which has the best available performance according to the results presented. This topic can therefore be researched further to determine what

Table 5: G3 and LT-modified G3 performance comparison.

System Specifications	$\frac{E_b}{N_0}$	G3 System	LT-modified G3 System	
			BP	GE
$N_{SYM} = 40$	-	-	-	-
$\lambda = 1/0.003$	16	$4 \cdot 10^{-3}$	$3 \cdot 10^{-1}$	$3 \cdot 10^{-1}$
$\lambda = 1/0.009$	16	$1.5 \cdot 10^{-4}$	$9.6 \cdot 10^{-2}$	$1.7 \cdot 10^{-1}$
$\lambda = 1/0.015$	13.5	$1.2 \cdot 10^{-4}$	$6.1 \cdot 10^{-2}$	$7.5 \cdot 10^{-3}$
$N_{SYM} = 56$	-	-	-	-
$\lambda = 1/0.003$	13	$2.2 \cdot 10^{-2}$	$3.6 \cdot 10^{-1}$	$3 \cdot 10^{-1}$
$\lambda = 1/0.009$	13	$6.3 \cdot 10^{-3}$	$2.3 \cdot 10^{-1}$	$1 \cdot 10^{-1}$
$\lambda = 1/0.015$	12	$1.8 \cdot 10^{-3}$	$1.7 \cdot 10^{-1}$	$1.1 \cdot 10^{-4}$
$N_{SYM} = 252$	-	-	-	-
$\lambda = 1/0.003$	13	$1.5 \cdot 10^{-3}$	$4.5 \cdot 10^{-1}$	$5 \cdot 10^{-1}$
$\lambda = 1/0.009$	12.5	$1.3 \cdot 10^{-4}$	$2.5 \cdot 10^{-1}$	$2.2 \cdot 10^{-1}$
$\lambda = 1/0.015$	9.5	$9.8 \cdot 10^{-2}$	$7.5 \cdot 10^{-2}$	$1.2 \cdot 10^{-3}$

the threshold conditions should be. It is theorised that the addition of a high rate LDPC code either as an outer code as is done in raptor codes [15] or as an inner code [16] would improve the performance problems in most cases but would also present the trade-off of adding further complexity.

4.3 System Complexity Comparison

Differences in complexity between the G3 and LT-modified G3 systems originate from the components that are not shared between them. Specifically, the differences in complexity reside in the LT code component which has been concatenated as the RS code, CC code and interleaver components are kept constant amongst implementations which use the same number of OFDM symbols N_{SYM}.

Encoding of LT codes is performed by the XOR of $O(\ln(\frac{k}{\delta}))$ input packets on average as this is the average degree of an encoded packet [12]. Each symbol XOR operation is composed of l individual XOR operations resulting in an encoding cost of the order $O(\log k)$ after simplification[53]. On the other hand for the decoder using BP, successful

decoding can be achieved by $k+O(\sqrt{k}\cdot\ln^2\frac{k}{\delta})$ received encoded symbols with probability $1-\delta$ which should require the XOR of $O(k\cdot\ln(\frac{k}{\delta}))$ packets on average [12]. In this case, due to the frame size limit this number of symbols is not reached in most cases and therefore decoding is usually performed with less operations. The upper bound of the average cost for the decoding process using BP is therefore of the order $O(k \log k)$. On the other hand, the decoder implementation with GE has an increased complexity where a matrix with k rows is solved with costs the order of $O(k^3)$ [61].

As can be seen from the analysis, concatenating G3 systems with an LT code increases performance under certain conditions but has the drawback of increasing complexity especially on the receiver side. The transmitter is considered to be of low complexity as XOR operations are cheap to perform. AMR systems are typically asymmetric as they are built as a network composed of several nodes (electrical/gas/water meters) communicating through the PLC channel with a centralised agent which then processes the data [62]. This can be seen as a star network topology. Modification through the use of LT codes would thus be well tolerated by the system as the receiver which has higher complexity would be implemented in the centralised agent component which possesses more available resources whilst only the transmitters with lower complexity would need to be installed on the individual meter nodes.

During the decoding process, another variable that needs to be considered is the delay brought on by the decoder. Specifically, decoding using GE can add considerable delay as decoding only starts once at least k packets have been received which are then all processed as a batch. Each time the process fails, a new received packet is added to the matrices and the whole GE process restarts again. It has been shown that this delay can be reduced by modifying the GE algorithm to process the received packet as they arrive and not restart the GE process when decoding is unsuccessful if more packets are still to be available [52, 63].

4.4 Conclusion from Simulation Results

It has been shown that current day systems provided by up-to-date standards such as the G3 standard can be improved under certain conditions by concatenating them with

a type of fountain code named LT code. This concept is demonstrated to successfully improve the performance of G3 systems, by providing a non-negligible coding gain in 2 of the 18 scenarios when using a GE LT decoder. An adaptive system is thus recommended which changes based on the channel conditions and which uses GE decoding with an optimal data rate based on the system used. The modification results in a complexity trade-off which is investigated. It is noted that the added complexity can be well tolerated considering that it resides mainly in the receiver and that in the context of smart grid AMR applications the receiver is the centralised system which possesses more available resources than the smaller units attached to the meters being monitored.

Chapter 5: Conclusion

5.1 Research Summary

This research centres around the question *"Can systems provided by current narrowband PLC standards be made more robust through the use of fountain codes, specifically LT codes, such that a new system operates at a similar or better bit error rate value and how does this modification affect the complexity of the system?"*. Firstly, the literature review is presented which examines what the various existing standards for narrowband PLC are, what the various methods for modelling the PLC channel are, what time diversity techniques exists and where they have been used in the context of PLC, and finally what methods exist for simulating PLC systems. This includes discussions on the advantages and disadvantages of each component as well as the reasoning behind the choices made for this research. Secondly in Chapter 3, background information is provided which allows for a better understanding of the research. This includes a description of all the individual components which are present in the PLC system such as the various FEC schemes, modulation techniques and channel model. From these components, two sets of systems are implemented where one is based on G3 systems operating in robust mode and the other set is based on a modification of the G3 systems which use an LT code as opposed to an RC code. Thirdly, the results of the paper which has been submitted to the *IEEE Transactions on Consumer Electronics* are shown in chapter 4. From these results, it is seen that it is indeed possible to improve some of the robust G3 systems through the use of LT codes provided that the channel impulse conditions are better than a certain threshold. Finally, a conclusion is drawn in this chapter.

5.2 Recommendations and Possible Future Work

Following the results of this research several new directions could be taken for the advancement of knowledge. Firstly, a physical implementation of the G3 and LT-modified G3 systems using the hardware mentioned in Section 2.4.1 could be used to verify the obtained results. Secondly, further test programs could be implemented to determine the exact λ threshold values at which point LT-modified G3 systems start being outperformed by the original G3 systems. This would give a boundary condition which the adaptive scheme could rely on following channel estimation. Thirdly, an LDPC code could be added to the FEC chain either before or after the LT code to determine whether the performance problem could be overcome. A further complexity analysis would then need to be performed on the modified system to identify what the new complexity trade-offs would be.

5.3 Conclusion

The answer to the research question *"Can systems provided by current narrowband PLC standards be made more robust through the use of fountain codes, specifically LT codes, such that a new system operates at a similar or better bit error rate value and how does this modification affect the complexity of the system?"* is as follows: Yes, current narrowband PLC standards can be made more robust through the use of LT codes using GE decoding with an appropriate code rate but not under worst case channel conditions. There exists an impulse rate parameter λ threshold value from which LT-modified G3 systems start being outperformed by the original G3 systems which use RC when comparing BER vs E_b/N_0 performances. Performing this modification does have a complexity trade-off as the addition of an LT encoder and decoder to the FEC chain increases complexity. It is observed that this complexity increase is more prominent on the receiver side as the transmitter component mostly uses the XOR operation which is not considered to be a costly operation. As this type of communication is typically used in AMR applications, the complexity can be well tolerated. This is due to the fact that AMR systems are usually built around a star network topology where a centralised receiver node which possesses more processing resources is connected to several measurement nodes which transmit data to it. The LT decoder would therefore be implemented on this centralised receiver whilst the measurement nodes with less

processing capability would only be fitted with an LT encoder. An adaptive scheme is thus recommended which makes use of either LT codes with GE decoding or an RC depending on the channel conditions.

References

[1] H.C. Ferreira and L. Lampe and J. Newbury and T.G. Swart, *Power Line Communications: Theory and Applications for Narrowband and Broadband Communications over Power Lines*. United Kingdom: John Wiley and Sons, 2010.

[2] B. Baraboi, "Narrowband powerline communication applications and challenges," Ariane Controls Inc, 2013.

[3] B.S. Park and D.H. Hyun, "Implementation of AMR system using power line communication," in *IEEE Transmission and Distribution Conference and Exhibition*, vol. 1, October 2002, pp. 18–21.

[4] B. Sivaneasan and E. Gunawan and P.L. So, "Modeling and performance analysis of automatic meter-reading systems using PLC under impulsive noise interference," in *IEEE Transactions on Power Delivery*, vol. 25 no. 3, March 2010, pp. 1465–1475.

[5] Y. Kim and J.N. Bae and J.Y. Kim, "Performance of power line communication systems with noise reduction scheme for smart grid applications," in *IEEE Transactions on Consumer Electronics*, vol. 57 no. 1, February 2011, pp. 46–52.

[6] Y-S. Son and K-D Moon and C. Kim, "Home energy management system based on power line communication," in *IEEE Transactions on Consumer Electronics*, vol. 56 no. 3, August 2010, pp. 1380–1386.

[7] T.A. Papadopoulos and C.G. Kaloudas and A.I. Chrysochos and G.K. Papagiannis, "Application of narrowband power-line communication in medium-voltage smart

distribution grids," in *IEEE Transactions on Power Delivery*, vol. 28 no. 2, April 2013, pp. 981–988.

[8] *PLC G3 Physical Layer Specification*, Electricity Reseau Distribution France Std. PLC G3 OFDM, 2008.

[9] *Air Interface for Fixed Broadband Wireless Access Systems*, IEEE Std. 802.16, 2004.

[10] L. Cheng and T.G Swart and C. Ferreira, "Adaptive rateless permutation coding scheme for OFDM-based PLC," in *IEEE 17th International Symposium on Power Line Communications and Its Applications*, March 2013, pp. 242–246.

[11] L. Cheng and H.C. Ferreira, "Time-diversity permutation coding scheme for narrow-band power-line channels," in *IEEE International Symposium on Power Line Communications and Its Applications*, March 2012, pp. 120–125.

[12] M. Luby, "LT codes," in *The 43rd Annual IEEE Symposium on Foundations of Computer Science*, 2002, pp. 271–280.

[13] P. Amirshahi and S.M. Navidpour and M. Kavehrad, "Fountain codes for impulsive noise correction in low-voltage indoor power-line broadband communications," in *3rd IEEE Consumer Communications and Networking Conference*, vol. 1, 2006.

[14] M. Luby and M. Watson and T. Gasiba and T. Stockhammer, "High-quality video distribution using power line communication and application layer forward error correction," in *IEEE International Symposium on Power Line Communications and Its Applications*, March 2007, pp. 431–436.

[15] A. Shokrollahi, "Raptor codes," in *IEEE Transactions on Information Theory*, vol. 52 no.6, June 2006, pp. 2551–2567.

[16] N. Andreadou and A.M. Tonello, "On the mitigation of impulsive noise in power-line communications with LT codes," in *IEEE Transactions of Power Delivery*, vol. 28 No. 3, July 2013, pp. 1483–1490.

[17] LandysGyr. (2015) Landis+Gyr brings G3 PLC smart metering to Austria. [Online]. Available: http://www.landisgyr.com/landisgyr-brings-g3-plc-smart-metering-austria-2/

[18] Elster Group GmbH. (2014) ERDF selects elster to support rollout of up to 35 million smart meters in France. [Online]. Available: http://www.elster.com/en/press-releases/2014/1823302

[19] J. Anatory and M.M. Kissaka and N.H. Mvungi, "Broadband services provision in powerline communications of developing countries," in *IEEE Symposium on Power Line Communications and Its Applications*, April 2005, pp. 376–380.

[20] *Signalling on low-voltage electrical installations in the frequency range 3 kHz to 148.5 kHz - Part 1: General requirements, frequency bands and electromagnetic disturbances*, CENELEC Std. EN 50 065-1, 2011.

[21] *PRIME Specification for PoweRline Intelligent Metering Evolution*, Iberdrola Std. Revision 1.4, 2014.

[22] *Narrowband orthogonal frequency division multiplexing power line communication transceivers for PRIME networks*, ITU-T Std. G.9904, 2012.

[23] *PRIME v1.4 White Paper*, Iberdrola Std., 2014.

[24] *Standard for Low Frequency (less than 500 kHz) Narrow Band Power Line Communications for Smart Grid Applications*, IEEE Std. P1901.2, 2013.

[25] O.G. Hooijen, "On the channel capacity of the residential power circuit used as a digital communications medium," *IEEE Communications Letters*, vol. 2 no. 10, June 1998.

[26] M. Katayama, "A mathematical model of noise in narrowband power line communication systems," in *IEEE Journal on Selected Areas in Communications*, vol. 24 no. 7, July 2006, pp. 1267–1276.

[27] O.G. Hooijen, "A channel model for the residential power circuit used as a digital communications medium," in *IEEE Transactions on Electromagnetic Compatibility*, vol. 40 no. 4, November 1998, pp. 331–336.

[28] J.-J. Lee and S.-J. Choi and H.-M. Oh and W.-T. Lee and K.-H. Kim and D.-Y. Lee, "Measurements of the communications environment in medium voltage power distribution lines for wide-band power line communications," in *International Proceedings on Power Line Communications and its Applications*, Zaragosa, Spain, 2004, pp. 69–74.

[29] J.E. Gilley, "Bit-error-rate simulation using matlab," Transcrypt International, Inc, Tech. Rep., August 2003.

[30] M.K. Simon and M.S. Alouini, *Digital Communication over Fading Channels - A Unified Approach to Performance Analysis*, 1st ed. Wiley, 2000.

[31] T. Shongwe and V.N. Papilaya and A.J. Han Vinck, "Narrow-band interference model for OFDM systems for powerline communications," in *17th IEEE International Symposium on Power Line Communications and Its Applications*, March 2013, pp. 268–272.

[32] J. Stensby, "Chapter 9: Commonly used models: Narrow-band gaussian noise and shot noise," Class Notes, 2013, eE603.

[33] M. Zimmermann and K. Dostert, "An analysis of the broadband noise scenario in powerline networks," in *IEEE International Symposium on Powerline Communications*, vol. 52 no. 4, September 2000, pp. 131–138.

[34] D. Middleton, "Canonical and quasi-canonical probability models of class A interference," in *IEEE Transactions on Electromagnetic Compatibility*, vol. EMC-25 no. 2, May 1983, pp. 76–106.

[35] D. Middleton, "Statistical-physical models of electro-magnetic interference," in *IEEE Transactions on Electromagnetic Compatibility*, vol. EMC-19 no.3, August 1977, pp. 106–127.

[36] D. Middleton, "Canonical non-gaussian noise models: Their implications for measurement for prediction of receiver performance," in *IEEE Transactions on Electromagnetic Compatibility*, vol. EMC-21 no. 3, August 1979, pp. 209–220.

[37] M. Zimmermann and K. Dostert, "Analysis and modeling of impulsive noise in broad-band powerline communication," in *IEEE Transaction on Electromagnetic Compatibility*, vol. 44 no. 1, February 2002, pp. 249–258.

[38] M. Zimmermann and K. Dostert, "A multipath model for the powerline channel," in *IEEE Transactions on Communications*, vol. 50 no. 4, April 2002, pp. 553–559.

[39] E.N. Gilbert, "Capacity of a burst-noise channel," *The Bell System Technical Journal*, pp. 1254–1265, September 1960.

[40] E.O. Elliott, "Estimates of error rates for codes on burst-noise channels," *The Bell System Technical Journal*, pp. 1977–1997, April 1963.

[41] B.D. Fritchman, "A binary channel characterization using partitioned markov chains," *IEEE Transactions on Information Theory*, vol. it-13 no. 2, April 1967.

[42] A.D. Familua and L. Cheng, "Modeling of in-house CENELEC A-band PLC channel using fritchman model and baum-welch algorithm," in *IEEE 17th International Symposium on Power Line Communications and its Applications*, March 2013.

[43] S. Lin and J. Costello, *Error Control Coding*, 2nd ed. New Jersey: Pearson Education Inc, 2004.

[44] M. Luby and A. Shokrollahi and M. Watson and T. Stockhammer and L. Minder, *Raptor Forward Error Correction Scheme for Object Delivery*, IETF Std. RFC 6330, 2011.

[45] M. Luby and A. Shokrollahi and M. Watson and T. Stockhammer, *Raptor Forward Error Correction Scheme for Object Delivery*, IETF Std. RFC 5053, 2007.

[46] A.D. Familua and A.R. Ndjiongue and K. Ogunyanda and L. Cheng and H.C. Ferreira and T.G. Swart, "A Semi-Hidden Markov Modeling of a Low Complexity FSK-OOK In-House PLC and VLC Integration," in *Proceedings of the IEEE International Symposium on Power Line Communications and its Applications*, Texas, USA, March 2015, pp. 199–204.

[47] A.D. Familua and R. Van Olst and K. Ogunyanda and L. Cheng and H.C. Ferreira and T.G. Swart, "Narrowband PLC Channel Modeling using USRP and PSK Modulations," in *18th IEEE International Symposium on Power Line Communications and Its Applications*, Glasgow, March 2014, pp. 156–161.

[48] Mathworks. (2016) Communication systems toolbox. [Online]. Available: http://www.mathworks.com/products/communications/

[49] Mathworks. (2016) Signal processing toolbox. [Online]. Available: http://www.mathworks.com/products/signal/

[50] M. Hochg, "Comparison of PLC G3 and PRIME," in *IEEE International Symposium on Power Line Communications and its Applications*, April 2011, pp. 165–169.

[51] T. Tirronen, "Optimal degree distributions for LT codes in small cases," Master's thesis, Helsinki University of Technology, Helsinki, Finland, November 2005.

[52] V. Boglio and M. Grangetto and R. Gaeta and M. Sereno, "On the fly gaussian elimination for LT codes," in *IEEE Communications Letters*, vol. 13 no. 12, December 2009, pp. 953–955.

[53] M.A. Guede, "Optimization of the belief propagation algorithm for Luby transform decoding over the binary erasure channel," Master's thesis, Delft University of Technology, Delft, Netherlands, July 2011.

[54] L.J. Deutschi, "The effects of reed-solomon code shortening on the performance of coded telemetry systems," in *TDA Progress Report*, 1983, pp. 14–20.

[55] W.C. Huffman and V. Pless, *Fundamentals of error-correcting codes*, 1st ed. Cambridge, United Kingdoms: Cambridge University Press, 2010.

[56] J. Lassing and T. Ottoson and E. Strom, "Packet error rates of terminated and tailbiting convolutional codes," in *The International Series in Engineering and Computer Science*, vol. 703, 2002, pp. 151–156.

[57] S. Haykin, *Communication Systems*, 4th ed. New York, United-States: John Wiley and Sons, 2000.

[58] T.K. Moon, *Error Correction Coding Mathematical Methods and Algorithms*, 1st ed. New Jersey: John Wiley and Sons Inc, 2005.

[59] J.G. Proakis and M. Salehi, *Communication Systems Engineering*, 5th ed. McGraw Hill, 2008.

[60] J.G. Proakis, *Digital Communications*, 2nd ed. Prentice-Hall, 2002.

[61] V.S. Ryaben'kii and S.V. Tsynkov, *A Theoretical Introduction to Numerical Analysis*, 1st ed. Chapman and Hall, 2006.

[62] C. Wei and J. Yang, "Implementation of automatic meter reading system using PLC and GPRS," in *Journal of Information and Computational Science*, vol. 8, 2008, pp. 4343–4350.

[63] S. Kim and K. Ko and S.Y. Chung, "Incremental gaussian elimination decoding of raptor codes over BEC," in *IEEE Communications Letters*, vol. 12 no. 4, April 2008, pp. 307–309.

Appendix A: Derivation of Inverse CDF Sampling Formula for Exponential Distribution

The PDF of the exponential distribution is defined as follows:

$$f_X(x) = \begin{cases} \lambda e^{-\lambda x} & x \geq 0 \\ 0 & x < 0 \end{cases}$$

The CDF of the exponential distribution can then be obtained by integrating the PDF

$$F_X(x) = P[X \leq x] = \int_{-\infty}^{x} f_X(x) = \int_{0}^{x} f_X(x) \tag{43}$$

$$\int_{0}^{x} f_X(t)dt = \int_{0}^{x} \lambda e^{-\lambda t} dt \tag{44}$$

$$\int_{0}^{x} \lambda e^{-\lambda t} dt = e^{-\lambda t}|_{0}^{x} = -e^{-\lambda x} - (-e^{-\lambda 0}) \tag{45}$$

Which results in

$$F_X(x) = \begin{cases} 1 - e^{-\lambda x} & x \geq 0 \\ 0 & x < 0 \end{cases}$$

Inverse CDF sampling functions by generating random samples uniformly distributed between 0 and 1 to then find the matching X along the curve. Let U be this uniformly generated random variable.

$$U = 1 - e^{-\lambda X} \tag{46}$$

$$1 - U = e^{-\lambda X} \tag{47}$$

$$\ln(1 - U) = -\lambda X \tag{48}$$

$$\ln(1 - U) = -\lambda X \tag{49}$$

$$X = -\frac{\ln(1 - U)}{\lambda} \tag{50}$$

Samples can then be generated by generating new samples U and substituting them into (50).